DESCRIPTION: State the application's broad, long-term objectives and specific aims, making reference to the health relatedness of the project. Describe concisely the experimental design and methods for achieving these goals. Avoid summaries of past accomplishments and the use of the first person. This abstract is meant to serve as a succinct and accurate description of the proposed work when separated from the application. **DO NOT EXCEED THE SPACE PROVIDED.**

PROJECT III: Determinants of Single-Cell Response to Electrical Stimulation

Project III investigates ways that spatial and temporal properties of intracochlear electrical stimuli define responses of first- and second-order auditory neurons. Recordings of auditory nerve fiber and anteroventral cochlear nucleus bushy cell activity will be obtained acutely in normal-hearing cats and in monaurally deafened cats with varying degrees of spiral ganglion survival. Neural responses will be analyzed quantitatively using two multi-channel intracochlear electrode designs and various electrical field-coupling configurations.

Experiments are subdivided into two major classes. The first class investigates effects of intracochlear current field geometry and summation on single-cell responses. In this, we will use an experimental 11-contact electrode to determine the effects of varying field coupling configurations on neural response threshold and rate of growth. We will also examine channel interactions produced by stimulating two electrode channels simultaneously. Late in the award period, similar experiments will be done using advanced electrodes developed in Project I.

The second class of experiments utilizes the same 11-contact array to investigate temporal, dynamic and stochastic aspects of single-cell response. Effects of varying the temporal structure of stationary and time-varying waveforms will be determined for pulsatile and sinusoidal signals, and the effects of neural refractoriness and discharge history will be examined using non-simultaneous masking paradigms. For both experimental classes, physiological data taken from deafened animals will be related to anatomic information about patterns of spiral ganglion survival and the detailed morphology of single cells.

Another component of Project III is the development of lumped-element and stochastic node models that will be used to predict single-cell responses to electrical stimuli and the anatomic dependencies of neural activity. The lumped-element models anticipate distributions of electrical potential within and around spiral ganglion cells, given a specified current field orientation and strength. The stochastic models use descriptions of neural node biophysics and morphology to predict neural response threshold, rate of response growth, and the temporal dispersion of the response.

Clinically relevant applications of the data collected in Project III include (1) defining the electrode configurations and stimulating waveforms that generate optimal responses, (2) exploring possibilities for exerting control over the spatial extent and temporal fine structure of the neural response, and (3) correlating neural response properties with detailed anatomic information on spiral ganglion survival.

KEY PERSONNEL ENGAGED ON PROJECT

NAME, DEGREE(S), SSN	POSITION TITLE AND ROLE IN PROJECT	DEPARTMENT AND ORGANIZATION
Eric Javel, Ph.D. 156-38-4421	Asst. Med. Res. Prof. Principal Investigator	Div. of Otolaryngology Duke Univ. Medical Center
Chris van den Honert, Ph.D. 028-42-3505	Senior Scientist Co-Investigator	Neuroscience Program Office Research Triangle Institute
Charles C. Finley, Ph.D. 420-66-4216	Senior Scientist Co-Investigator	Neuroscience Program. Office. Research Triangle Inst.
Mark W. White, Ph.D. 508-60-4200	Associate Professor Co-Investigator	Dept. Electrical/Computer Eng. North Carolina State Univ.
C. Daniel Geisler, Sc.D.	Professor Consultant	Dept. of Neurophysiology Univ. of Wisconsin Medical School

INTRODUCTION

The site visit team criticized our original proposal for Project III on five counts. These, and the remedies we have implemented, are as follows:

1. The manpower is insufficient to carry out all the proposed work. This point was well taken. Since the time of the site visit, Chris van den Honert, a physiologist/engineer with extensive experience in single-cell recordings under conditions of cochlear implantation and electrical stimulation, has been recruited into this PPG. He will devote 20% effort to Project III, where he will be responsible for the studies involving spatial effects of electrical stimulation. The inclusion of Dr. van den Honert significantly improves our ability to collect and analyze physiological data, and it also allows Dr. Javel to contribute more time (25% effort) to Project III. Dr. Javel will be responsible for the studies involving temporal and dynamic neural response properties. With the exception of Dr. Altman, whom the site visit team recommended be removed from Project III, all other personnel have been retained. We believe that manpower is now sufficient to accomplish the Project's goals.

2. The scope of the project is overly ambitious, given all the stimulus manipulations being done for three electrode types in both normal and deafened animals, . We have reduced the scope of the project by re-defining the stimulus conditions to be investigated and reducing the number of electrode types to be employed. A fact that did not come out in the site visit, but which is implicit in auditory nerve studies, is that the number of conditions investigable for any given fiber is constrained by the available data collection time, which is about 10-15 minutes. In the anteroventral cochlear nucleus (AVCN), however, the available recording time is considerably longer, and many stimulus conditions can be studied for each cell. Since our data collection apparatus can be set up to present signals and record responses without user intervention, we can easily expect to be able to present at least 5 conditions per fiber, and many more per AVCN cell. The application now makes it clearer how stimulus manipulations will be preselected to accommodate limitations on recording time. Also, we now note that only two electrode designs, namely the 11-contact and advanced electrodes described in Project I, are needed to collect the data we want. Descriptions of experiments have been re-cast accordingly. Finally, binaural deafening has been ruled out as a needed technique, and recordings from nuclei more central than AVCN will only be obtained as a last resort.

3. Experimental design and data analysis methods are described only superficially, and details such as the negation of electrophonic effects and the analysis of collision experiments have not been taken into consideration. In the original application, the amount of text devoted to experimental design and data analysis was constrained by NIH limitations on overall length. Faced with the problem of describing how our prior work led to this proposal and also listing in adequate detail all the manipulations we intend to do, we elected to emphasize prior progress and experience at the expense of detailed descriptions of experiments. Apparently this was a mistake. The application now devotes more text to descriptions of experiments, the kinds of analyses that will be performed, and pitfalls that can arise in interpreting the findings. Also, the relationships of model predictions to neural data, as well as the specific hypotheses being tested, are spelled out more clearly.

At the site visit, we noted that the originally-proposed experiments utilizing spike collision to determine spike excitation site will not work. Accordingly, these studies have been dropped from the proposal. Any inferences about spike initiation will be drawn indirectly from anatomic data and by correlating physiological responses with predictions made by the single-neuron models.

4. Data are not provided to support the assumption that responses of cells in the electrically stimulated auditory nerve and AVCN are directly comparable. We have added text describing the effects of temporal summation in intracellular recordings from AVCN, and we now identify the conditions under which auditory nerve and AVCN data may be compared. Briefly, we expect that the effects of temporal summation will be negligible for bushy cells because of the high efficacy of the end-bulb synapse and the high degree of synchronization among input auditory nerve fiber discharges. Based on known tuning properties of AVCN cells, we also expect spatial summation effects to be negligible. Stellate cells, whose responses are distinguishable from bushy cells on the basis of action potential waveshape, the temporal structure of the PST histogram at near-threshold intensities, and the lack of a pre-potential, will be excluded from study because prior work has shown that temporal summation effects are likely to be significant for these cells.

We noted at the site visit that unpublished work done by us and by others indicates that response properties of bushy cells to intracochlear electrical stimuli are very similar to those recorded in the auditory nerve. However, because this conclusion is based only on cursory examination of data collected in response to pulsatile stimuli only, we will perform a study to compare responses of similarly-tuned AVCN and spiral ganglion cells to identical electrical stimuli. The purpose of this work is to determine whether any differences exist in input-output relationships and temporal fine structure of these cells' responses, and to determine the nature and magnitude of transforms occurring at the cochlear nerve synapse. We expect these effects to be minimal.

5. Data to support the contention that characteristic frequencies (CFs) can be determined for neurons in deafened ears were not convincing. Results shown at the site visit indicated that the contralateral acoustic masking technique used in this procedure has merit; however, those data only showed a general effect which did not allow CF

to be determined accurately. We are in the process of tooling up to repeat this experiment using more appropriate maskers. Information about the outcome of that effort will be submitted as a supplement. We have also performed modeling work to show how CF can be estimated using bandpass maskers, which were the ones used in our initial study. Although the model succeeded in estimating CF reasonably accurately, we recognize the fact that this model is exceptionally sensitive to small changes in the slopes of the masking functions. This suggests that bandpass maskers will not provide reliable information about CF. Also, we now list four alternative strategies to estimate CF if the masking technique fails to provide us with the appropriate information.

Minor changes made to the text that follows have not been identified. Paragraphs printed in bold letters either are new or have undergone extensive revision since the previous submission.

A. Specific Aims

The intent of Project III is to identify and study mechanisms that govern threshold and suprathreshold responses of single auditory neurons to intracochlear electrical stimulation. Following an initial study to determine the degree to which auditory nerve fiber responses correlate with AVCN bushy cell responses obtained from similarly-tuned cells, the next three years of the award period will be devoted to studying responses of auditory neurons in intact and deafened cats using a single electrode design that allows the selection of several field coupling configurations. Experiments have been designed such that the data they provide can be used to test predictions of lumped-element and stochastic models of intracochlear current distribution and neural response. Implicit in all studies is the desire to address scientific issues pertinent to the clinical application of cochlear implants. Among these are (1) determining the electrode configurations and stimulating waveforms that generate optimal responses, (2) examining possibilities for exerting control over the spatial extent and temporal fine structure of the neural response, and (3) correlating neural response properties with detailed information about cochlear and spiral ganglion cell morphology. Of particular interest is exploring possibilities for using specialized stimulation schemes to better approximate neural response patterns observed in acoustic hearing. General goals and specific objectives of Project III are as follows:

1. <u>To determine how current field orientation and summation influence single-cell response</u>. Cats with previously normal hearing and cats with experimentally induced unilateral deafness of variable duration will be implanted acutely with 11-contact point-source electrode arrays of the type described in Project I. Responses of auditory nerve fibers and AVCN bushy will be collected as current field size and shape are systematically varied by re-assigning the electrodes used for current source and sink. Analyses will focus on quantifying relationships between neural response behavior and parameters associated with the stimulating field, and on developing single-neuron models of electrical excitability that predict neural response behavior. Specific objectives are as follows:

a. To compare neural response sensitivity and rate of growth for radial, longitudinal and offset-radial bipolar field configurations, and monopolar field configurations.

b. To collect detailed input-output functions using a variety of pulsatile and sinusoidal signals, in order to quantify interactions between field geometry and stimulus type.

c. To relate single-cell responses to the predictions of lumped-element and stochastic node models.

d. To determine the effects of current field summation caused by simultaneously presenting stimuli on two different electrode channels.

e. To correlate physiological and morphological data obtained from anatomically normal ears with identical data obtained from damaged ears, to test the hypothesis that patterns of intracochlear current spread differ in normal and deafened ears.

2. <u>To examine temporal, dynamic and stochastic properties of neural responses to electrical stimuli</u>. Temporal discharge patterns of auditory nerve fibers and bushy cells will be analyzed as the fine structure of stimulating waveforms is varied systematically along several dimensions. The general goals of these experiments are to determine which stimuli generate optimal neural responses, characterize the temporal fine structure of the response, and indirectly estimate the active site(s) of spike initiation. Specific objectives are as follows:

a. To determine effects of temporal waveshape on quantitative aspects of single-cell response, using stimuli consisting of monophasic, multiphasic and asymmetric rectangular pulses, sinusoids, pulses with variable rise times, and amplitude modulated signals.

b. To investigate the effects of stimulation rate/frequency, intensity and signal polarity on neural response sensitivity and temporal fine structure.

c. To examine stochastic properties of neural response using signals consisting of bandpass noise and variable-duration pulses, and relate these to the predictions of passive and active membrane models.

d. To quantify the effects of refractoriness and discharge history on cell responsiveness using non-simultaneous masking techniques. Stimulus parameters to be varied include the cochlear locus of the masker, the time interval between masker and probe, masker type and duration, and overall intensity.

e. To compare data obtained from normal ears with identical data obtained from deafened ears, for the purpose of testing the hypothesis that temporal neural response characteristics vary as a function of spiral ganglion cell morphology.

B. Background and Significance

1. Introduction

Cochlear implants were put into use in human patients well in advance of detailed knowledge of the ways they operate on the neural level. Although successful development of cochlear implants is of obvious clinical importance, relatively few investigators are involved in studying the ways these devices operate. Fewer still are concerned with developing new, optimized electrode designs and generating speech processing strategies that elicit physiologically accurate patterns of neural responses. A considerably greater degree of understanding is clearly needed on several levels if the clinical goal of improved speech perception is to be achieved. Probably the most pressing needs from a basic research point of view are (1) determining quantitative relationships between stimulus waveform parameters and neural response, (2) gaining a detailed understanding of the effects of electrode geometry on current fields and neural excitation processes, and (3) determining the physiological and biophysical consequences of variable spiral ganglion survival.

2. Response Types and Site of Action Potential Initiation

Moxon (1971) was the first to provide detailed descriptions of auditory nerve fiber responses to electrical stimulation of the cochlea. Using a monopolar electrode placed on the round window of cats, he classified responses as direct-excitation ("alpha") and electrophonic ("beta") types on the basis of response latency and suprathreshold behavior. Further work done by van den Honert and Stypulkowski (1984, 1987), Hartmann *et al.* (1984), Hartmann and Klinke (1989), Parkins and Columbo (1987), Javel *et al.* (1987) and Javel (1989) verified Moxon's observations and extended them for stimulus waveforms consisting of sinusoids and both monophasic and biphasic pulses, and to bipolar electrode configurations. To summarize these authors' findings, direct excitation of spiral ganglion cells produces short-latency, highly synchronized action potentials. Responses can occur at any of 4 discrete latencies. The two shortest latencies, termed **A** and **B** by Javel, are clearly the result of direct excitation of spiral ganglion cells. The longest-latency or **D** response is probably generated by mechanical activation of the basilar membrane, either as the result of electrical stimulation and subsequent contraction of outer hair cells, or by traveling waves generated by charges differentially repelling or attracting the basilar membrane. Because **D** responses do not exist in deafened cochleas, they are unlikely to be of clinical significance. The origin of **C** responses is less clear: Their latencies are consistent with both direct excitation of inner hair cells and direct excitation of unmyelinated, slow-conducting peripheral processes of spiral ganglion cells. If the latter is true, which we feel is the case, then the **C** response can be treated as the "tail" of the **B** response.

Responses with both **A** and **B** latencies may co-exist in the same spike train at certain intensities, but only when biphasic pulses are used as stimuli (Javel *et al.*, 1987; van den Honert and Stypulkowski, 1987). The typical response progression is that longer-latency (450-800 uS) spikes are abruptly replaced by shorter-latency (300-450 uS) spikes, usually at a fairly high intensity. Monophasic pulses, on the other hand, generate spikes that group around only one latency regardless of intensity, and the latency that is observed often depends on pulse polarity (*i.e.*, direction of current flow).

Like responses to biphasic pulses, responses to low-frequency sinusoids can occur at multiple latencies, either on the anodic and/or the cathodic half-cycle (Hartmann *et al.*, 1984; Parkins and Columbo, 1987). Responses occurring during one half-cycle can be superseded by responses occurring during the other at high intensities, and spikes can be elicited on both the rising and the falling phases of a single half-cycle (van den Honert and Stypulkowski, 1987). For both sinusoidal and pulsatile stimuli, discharge phase-locking is strong even at near-threshold intensities. Interestingly, synchronization is somewhat poorer for low-frequency sinusoids than for narrow pulses presented at a similar rate. This suggests that the time course of charge delivery has a substantial impact on neural response and, presumably, on stimulus coding.

Javel *et al.* (1987) suggested that the two short latencies (**A** and **B**) correspond to direct excitation of the peripheral and central processes of the spiral ganglion cell. Van den Honert and Stypulkowski (1984, 1987) did not observe abrupt latency shifts using monophasic pulses but observed the phenomenon using biphasic pulses. They contended that the cell body does not necessarily reside between the spike initiation sites. In their view, the site of

spike initiation depends only on the position of relative depolarization, and different electrical field configurations can change this site's position. Whether or not this statement is true has not been determined, but this view is inconsistent with findings in modeling work done by us (White *et al.*, 1987; Finley *et al.*, 1987), which shows that the site of action potential initiation affects response threshold and dynamic range. This work also indicates that the cell body potentially plays an important role in determining response latency. Clearly, the issue of cell body effects is still open.

Related to the issue of spike latency and initiation site is the existence of current paths that extend radially across the modiolus and vertically into adjacent cochlear turns. Although it has been suggested that such paths exist, the conditions under which transmodiolar current spread occurs have not been determined fully. Without this knowledge we cannot understand the basis of channel interactions and current field summation, particularly in cases of poor nerve survival.

3. Temporal Response Properties

Discharges elicited by direct excitation of spiral ganglion cells are highly phase-locked from threshold (Hartmann *et al.*, 1984; van den Honert and Stypulkowski, 1984; Hartmann and Klinke, 1989; Javel, 1989). Values for synchronization index obtained in response to electrical stimuli usually exceed 0.85 for all stimulus types, whereas values observed in response to acoustic signals seldom exceed 0.90, and then only at very low stimulus frequencies. Synchronization to electrical sinusoids can be lower than synchronization to pulses (Hartmann *et al.*, 1984), and synchronization is observable to at least 12 kHz (Dynes *et al.*, 1989; Hartmann and Klinke, 1989).

In general, we have a good understanding of the synchronization behavior that can be expected from auditory nerve fibers responding to biphasic pulses and low-frequency sinusoids. However, this is where our knowledge stops. Except for rudimentary examinations of refractoriness and temporal integration, no one has ever conducted a parametric study of the ways that temporal waveform properties influence neural responses, and no one has thoroughly investigated discharge synchronization in nuclei more central than the auditory nerve. With regard to the latter, Clopton and Glass (1984), Glass (1984, 1985), and Clopton *et al.* (1989) have all demonstrated high degrees of phase-locking to electrical sinusoids and pulses in responses of cochlear nucleus cells.

Using a different preparation, Oertel (1985) and Oertel *et al.*(1989) have shown that bushy cells in AVCN, which possess end-bulbs of Held, respond differently to electrical stimulation of the auditory nerve than do stellate cells. In particular, bushy cells exhibit almost a one-for-one relationship between input spikes in the auditory nerve and postsynaptic spikes, whereas stellate cells (after the initial spike) exhibit various degrees of temporal summation, depending on stimulus intensity. Also, bushy cells respond with "primary-like" post-stimulus time (PST) histograms to brief tone pips, whereas stellate cells respond with "chopper" PST histograms (Rhode *et al.*, 1983a). Cells in dorsal cochlear nucleus, on the other hand, exhibit complex temporal response patterns, both to acoustic and electrical stimulation (Young and Brownell, 1976; Young and Voigt, 1982; Rhode *et al.*, 1983b).

Based on known temporal response properties of the various cell types in the cochlear nucleus, it is clear that the only cell group whose responses are relatively uncontaminated by synaptic arrangements and inhibitory influences are the bushy cells. Although stellate cells do not need inhibitory inputs to produce their stereotyped responses (Young, 1988), the presence of significant inhibitory influences cannot be ruled out.

4. Dynamic Response Properties

Dynamic response properties of electrically stimulated auditory neurons (adaptation, effects of waveform envelope modulation, etc.) are very poorly understood. Limited data were reported by Glass (1984) and Clopton and Glass (1984) on responses of cochlear nucleus neurons to two-component sinusoids presented electrically. They found that responses generally arise to the highest amplitude waveform peak and that the temporal fine structure of period histograms is a nonlinear function of intensity. Similarly, data obtained by us using amplitude-modulated pulse trains (see Preliminary Studies) suggest that spiral ganglion cells are exceptionally sensitive to small fluctuations in waveform envelope amplitude. Although it is quite obvious that nonlinear processes intrinsic to the spiral ganglion cell itself control this behavior, these processes are not well understood.

The absence of knowledge about dynamic response properties of electrically stimulated auditory neurons is something that must be corrected because (1) dynamic response properties are known to be important in coding many speech consonants, (2) electrical signals delivered to "analog" implants (e.g., the Symbion device) often possess marked stimulus envelopes, and (3) recent findings with non-simultaneous, high-frequency, amplitude-modulated electrical stimuli have shown that certain patients derive considerable benefit, in terms of improved speech recognition, from the use of complex modulated signals (Wilson, personal communication).

5. Input-Output Relationships

Rate-intensity functions of electrically stimulated neurons have been described by Javel *et al.* (1987) for pulsatile signals and by Hartmann *et al.* (1984) and Hartmann and Klinke (1989) for sinusoids and pulses. These always possess rapid rates of growth that are power functions of current level, and they possess saturation discharge rates that are highly correlated with stimulus frequency. In agreement with the predictions of stochastic models (White *et al.*, 1987), dynamic ranges of electrically stimulated auditory nerve fibers are usually <6 dB, and short-latency responses ostensibly initiated on the central processes of spiral ganglion cells have smaller dynamic ranges and higher thresholds than responses initiated on peripheral processes.

Interestingly, the probability of spike generation appears, at least for pulsatile stimuli, to be nearly constant at a given intensity, regardless of the signal frequency employed (Javel, 1989). This has two implications: The first is that dynamic range is directly related to stimulus frequency and depends on virtually no other stimulus-related factor; and the second is that tuning curves for pulsatile signals are flat. Interestingly, tuning curves for sinusoids can show the same frequency dependence that is often observed behaviorally for the same signals (Hartmann and Klinke, 1989; Pfingst, 1989). The basis of the difference between tuning properties for pulsatile and sinusoidal signals is unknown.

Javel (1989) and Hartmann and Klinke (1989) found that electrically elicited discharges are non-stochastic at suprathreshold intensities. That is, discharges occurring at a given rate tend strongly to cluster at times corresponding to the inverse of rate, regardless of stimulus frequency. Although initial modeling work has been done (White, 1984) to suggest how these responses might come about, the implications of deterministic response behavior for perceptual codes is unclear.

Changing the width of a pulsatile stimulus produces predictable changes in response threshold (van den Honert and Stypulkowski, 1984; Parkins and Columbo, 1987; Javel *et al.*, 1987). Strength-duration curves indicate that spiral ganglion cells have variable chronaxies that are somewhat longer than those predicted by traditional neural membrane models (e.g., McNeal, 1976). Also, response threshold exhibits constant-charge behavior for all but very long pulsewidths (Liang, 1988). Although these findings suggest that the effects of temporal integration should be generally predictable in the electrically stimulated auditory nerve, the appropriate tests have not been done.

6. Intracochlear Current Spread

Using monaurally deafened cats and recording from binaurally sensitive cells in the inferior colliculus, Merzenich *et al.* (1973) and Merzenich and White (1977) determined that bipolar electrode configurations generate excitation patterns that are confined to relatively restricted cochlear regions in the vicinity of the stimulating electrodes, and that monopolar configurations excite neurons over a broad range of characteristic frequencies (CFs). Extending these findings, van den Honert and Stypulkowski (1987) determined that radial bipolar electrode configurations produced more restricted excitation patterns than either longitudinal bipolar or monopolar configurations. Liang (1988) used a somewhat different electrode design and obtained data that were similar to but not nearly as "clean" as those obtained by van den Honert. Hartmann and Klinke (1989) used a Nucleus-type banded electrode to obtain data indicating even less localization than that obtained by van den Honert for longitudinal bipolar electrodes, but the values of space constants were similar to those reported by Black and Clark (1980) and Finley *et al.* (1989) for banded electrodes. Importantly, all localization data reported to date deal only with threshold responses: There is no description in the literature of excitation patterns at suprathreshold intensities. It is the suprathreshold responses, of course, that are of importance for speech perception.

Along with neural survival, the degree of response localization and crosstalk among stimulated electrodes (commonly known as channel interactions) are widely considered to be the principal determinants of perceptual performance with cochlear implants. Because these aspects of intracochlear stimulation strongly impact both electrode designs and speech processing strategies, obtaining a detailed knowledge of them remains a critically important task, both in terms of understanding the perceptual performance capabilities of existing implantees and in terms of designing better implants.

7. Determinants of Response Threshold

Once acoustic sensitivity is lost, the spiral ganglion exhibits various degrees of degeneration that range from good survival to very poor survival. Degeneration appears to be an ongoing process that in cats occurs over several months or years (Leake and Hradek, 1988). The factors underlying the degree and rate of spiral ganglion degeneration are unknown, but degeneration seems to be accelerated by even slight trauma, for example during implant electrode insertion (Simmons, 1967; Shepherd *et al.*, 1985). Nothing is known about differences or similarities in the degenerative process in young versus adult subjects.

The only extensive work attempting to correlate auditory nerve survival with perceptual behavior has been done by Pfingst and his co-workers (Pfingst *et al.*, 1981, 1985; Pfingst and Sutton, 1983; Pfingst, 1989). They found that high behavioral thresholds are correlated with severe spiral ganglion damage, and that animals with good auditory nerve survival possess behavioral thresholds that are lower for sinusoids than for pulses. Importantly, the

shape of the frequency-threshold curve varies with nerve survival, being somewhat U-shaped in cases of good survival and relatively flat in cases of poor survival.

Using sinusoidal stimuli, Hartmann *et al.* (1984) obtained tuning curves from auditory nerve fibers of acutely implanted cats. Their data indicate that, like data from the most sensitive humans and monkeys, some fibers are most sensitive at 100 Hz and exhibit thresholds which increase with frequency. Other fibers, however, exhibit relatively flat tuning curves. Our own work (see Preliminary Studies) has shown that frequency-threshold curves obtained from single fibers are always flat for pulse stimuli, regardless of the degree of nerve survival.

Pfingst has shown that the most sensitive single-cell thresholds are still higher than behavioral thresholds. This suggests that threshold depends on temporal integration across a number of fibers. If so, then stochastic neural response properties (White *et al.*, 1987) play an important role in determining threshold. Despite suggestions that integration across neurons' responses is required to account for response threshold, the appropriate physiological studies have not been performed.

Despite the relative lack of pertinent physiological data, various membrane models have been proposed that predict magnitudes and temporal characteristics of neural responses to electrical stimuli (*e.g.,* Hill, 1936; Hodgkin and Huxley, 1952; Verveen, 1962; MacNeal, 1976). More recently, the principles employed by these models have been applied to the question of excitation by intracochlear electrical stimuli (White, 1984; Motz and Rattay, 1986; Finley *et al.*, 1987; White *et al.*, 1987; Finley, 1989). These findings are described in the Preliminary Studies.

8. Conclusions

Although a fair amount is known about responses of first-order auditory neurons to electrical stimuli consisting of single-frequency sinusoids and pulses with elementary waveshapes, the state of knowledge about the various temporal and spatial determinants of single-cell responses to intracochlear electrical stimulation is demonstrably inadequate. While single-cell responses in the electrically stimulated cochlea are simpler than activity patterns of acoustically driven neurons, complete descriptions of the ways that stimulus and electrical field parameters define responses of auditory neurons are lacking.

Despite their simplicity relative to most other neurons, spiral ganglion cells possess anatomic features that complicate descriptions of the ways they respond to intracochlear electrical stimulation. Better and more detailed information is obviously needed to determine (1) how stimulus parameters govern neural response, (2) how electrode and field geometry affect single-cell responses, (3) how variable nerve survival impacts the extent of intracochlear current fields and the response properties of active neurons. Until such information is available, designs for electrode arrays and algorithms for speech processing will remain suboptimal.

C. Preliminary Studies

Over the past several years the investigators in this project have conducted physiological studies to collect and analyze auditory nerve fiber responses to electrical signals presented through banded and point-source cochlear implants, and field and neural modeling studies to characterize intracochlear current spread and predict neural excitability. Although these studies relate to one another, they were undertaken independently, *i.e.*, before our research group formed. Because of this, progress in each area will be presented separately. Figures referred to are provided in an appendix.

1. Physiological Studies (Javel)

Specific aims of work done to date have been to (1) characterize the fine temporal structure of fiber responses to pulsatile stimuli, (2) quantify input-output relationships between stimulus intensity and discharge rate/synchronization, (3) determine how stimulus waveshape and modulation affects fiber responses, and (4) compare responses obtained from deafened animals with responses obtained from normal hearing animals. What follows here is a synopsis of some of the highlights of the physiological data we have collected thus far, emphasizing only those results that have not yet been published. The list of findings described below is by no means exhaustive.

Response Temporal Fine Structure. One of our earliest findings (Javel *et al.*, 1987) was that action potentials may arise at any of four latencies with respect to the onset of a biphasic pulse. These are indicated in the lower frame of Fig. 1, which shows period histograms obtained for acoustical sinusoid and electrical pulse stimuli. We have tentatively associated electrical response times, in increasing order of latency, with direct initiation of action potentials at the spiral ganglion cell's axon (**A** response), direct activation of the cell's peripheral process (**B** response), electrical excitation of the hair cell or the unmyelinated peripheral process of the spiral ganglion cell (**C** response), and mechanical activation of the basilar membrane with subsequent excitation of hair cells (**D** response).

The shortest-latency or **A** response occurs primarily at high stimulus intensities, is distributed very tightly in

time, and shows little adaptation. The **B** response is distributed more loosely but is still considerably more highly phase-locked than responses to acoustic stimuli. It usually possesses a lower threshold and exhibits adaptation-like behavior. **B** responses are often replaced by **A** responses at high (>1 mA) stimulus intensities, and at certain intensities both long- and short-latency responses may be observed in the same spike train. Fig. 2 shows period histograms in which this abrupt latency shift is evident.

Carrying the study of the latency shift phenomenon further, we compared responses obtained using biphasic pulses with responses obtained using monophasic pulses. These data indicate that both the anodic and cathodic phases of the biphasic stimulus are capable of exciting the neuron, that the excitation likely occurs at different points on the neuron's surface, and that the two phases may exhibit different response sensitivities. Spontaneous discharges, when present, had no effect on the **B-A** transition: The latency transition was observed in fibers with no spontaneous activity as well as in fibers with high spontaneous rates, and the general behavior of the latency transition was identical in all fibers.

An interesting observation that deserves more study pertains to the nature of the spike waveforms when **B-A** latency transitions occur. In all fibers studied to date, **A**-latency spikes were of significantly smaller amplitude than **B**-latency spikes, but the spike waveshapes were identical. Although the meaning of this phenomenon is unclear, the existence of two distinctly different spike amplitudes coexisting in the same spike train suggests that spike initiation and propagation mechanisms might be different for cathodic and anodic current, or that spikes are initiated at different sites along the length of the spiral ganglion cell.

We found, in situations where long- and short-latency responses coexist, that responses occurring near the beginning of a pulse train tend to be of the short-latency variety, whereas responses occurring later (*i.e.*, >50 mS after signal onset) tend to be of the longer-latency type. An example of this phenomenon is shown in Fig. 3, which shows dot-raster displays obtained at several intensities in response to biphasic pulse trains presented at a rate of 200 pulses/S. Other data we possess indicate that the time at which the latency transition occurs depends on intensity and pulse rate. Also, the initial phase of the stimulus (*i.e.*, anodic vs. cathodic) can play an important role in determining whether a latency transition occurs. Representative data are shown in Fig. 4, which indicates dot rasters obtained for initially anodic (left column) and initially cathodic (right column) pulses. In addition to a difference in absolute sensitivity, the data show that the intensity at which the initially cathodic pulses caused an **A**-latency response to occur (if one occurs at all) is considerably higher than the intensity that caused initially anodic pulses to elicit short-latency spikes. Despite its existence, the perceptual significance of the latency transition remains unclear.

Retention of Acoustic Sensitivity. Acute placement of a cochlear implant into scala tympani of a cat with normal hearing did not compromise acoustic sensitivity, tuning curve sharpness, or spontaneous discharge rates during the course of a 3-4 day experiment. Of particular importance is that acoustic sensitivity is normal even in the region of the cochlea occupied by the implant. In our studies the implanted array extended 8 mm into the cochlea, or to the 10-12 kHz region. Acoustic tuning curves of fibers tuned to these and higher frequencies exhibited normal thresholds and sharpness for the duration of the 3-4 day experiments.

Input-Output Relationships. Rate-intensity functions of auditory nerve fibers stimulated with biphasic pulse trains presented at different frequencies exhibit similar threshold sensitivities and rates of growth. Thus, within the dynamic range only stimulus intensity, not stimulus frequency, determines discharge rate. Maximum discharge rate is typically at the stimulus pulse rate, even for rates >800/S, and dynamic range is a strict function of stimulus pulse rate. At low discharge rates, rate-intensity functions obtained at different pulse rates virtually overlie, with fibers exhibiting a slight tendency to be more sensitive to high pulse-rate signals. High stimulus pulse rates cause responses to saturate at higher discharge rates, with an accompanying increase in dynamic range. Representative data are shown in Figs. 5 and 6.

We found that growth of discharge rate is almost always a power function of peak stimulus current and that variations in stimulus pulsewidth produce predictable changes in response sensitivity. These findings suggest that the most important factor in determining degree of excitation is the amount of electrical charge each pulse delivers. We also found that spikes are highly phase-locked to pulse stimuli, even at perithreshold intensities, and that response latencies are monotonic functions of intensity. **B**-latency responses always underwent a larger latency shift with increasing intensity than **A**-latency responses (Fig. 7).

Similar to perceptual data from human subjects with cochlear implants, dynamic ranges of rate-intensity functions obtained from electrically stimulated auditory nerve fibers vary from <1 dB to >7 dB at a 200/S pulse rate. A histogram showing the distribution of dynamic ranges obtained at this pulse rate is provided in Fig. 8. Consistent with the behavior of rate-intensity functions, we also found that dynamic ranges are correspondingly lower at lower pulse rates and higher at higher pulse rates, and they are slightly rising functions of threshold (Fig. 9). Although the identity of neural processes governing dynamic range is still uncertain, modeling studies (White *et al.*, 1987) suggest that dynamic range and rate of response growth are related to the diameter and internal resistance of the node of Ranvier at which spike initiation occurs. The data we have collected thus far strongly support the predictions of the modeling work.

Spike Timing. We found that discharges are highly synchronized to the pulse cycle at all suprathreshold

intensities and that the dynamic range for synchronization of non-electrophonic responses is typically <1 dB. Also, synchronization indices are much higher for biphasic electrical pulses than for either acoustic or electrical sinusoids. The high degree of synchronization and concomitant lack of temporal dispersion are indicated by the data in Fig. 10, which shows standard deviations of peaks of inter-spike interval histograms for electrical and acoustic signals presented to different fibers, plotted as a function of pulse rate. Although temporal dispersion for both signal types decreases with frequency, standard deviations of the electrical data are up to 5 times smaller than comparable acoustic data at low frequencies. The discrepancy increases as frequency increases.

Interestingly, we found that at all stimulus pulse rates, spikes tend to occur at regular time intervals equal to the reciprocal of discharge rate. This situation, which is reminiscent of acoustic responses to amplitude modulated tones, differs from acoustic responses to pure tones, wherein ISIs are distributed over a much broader range of time intervals. An example of this is shown in Fig. 11, which consists of ISI histograms obtained for pulse trains presented at different frequencies but at identical intensities.

Frequency Selectivity. "Tuning curves" for pulsatile stimuli (threshold as a function of pulse rate) are remarkably flat. An example is shown in Fig. 12. For pulse rates >500/S this curve resembles threshold sensitivity curves obtained for cochlear implants that deliver sinusoidal stimuli, but for low frequencies it does not. These findings also indicate that the spatial processing which is a hallmark of cochlear responses to acoustic stimuli must be provided by implant speech processors, i.e., the electrically stimulated auditory nerve possesses no inherent frequency selectivity.

Manipulations of Electrical Waveshape. We studied auditory nerve fiber responses to electrical stimuli whose stimulus waveshapes were systematically varied. These experiments were done to determine which waveforms produce the greatest dynamic ranges and lowest thresholds, and to determine which waveshapes are best suited, from a stimulus-response point of view, for use in interleaved-pulse stimulation strategies.

Fibers typically exhibit greatly decreased sensitivity to triphasic waveforms, that is, charge-balanced waveforms in which one phase (either the cathodic or the anodic) is broken into two segments that straddle the segment with opposite polarity. The amount of sensitivity decrease is a monotonic function of the duration of the initial stimulus phase. An example is shown in Fig. 13. As the temporal position of the cathodic phase shifts from one end of the pulse to the other, the rate-intensity function shifts toward higher intensities by almost 2 dB, and then shifts back again. One interpretation of the data shown is that the anodic phase of the stimulus hyperpolarizes the cell, and that the hyperpolarization must be overcome by the cathodic phase before excitation occurs. The data suggest that triphasic waveforms are clearly undesirable if maximizing sensitivity is important.

Another waveshape manipulation we performed consisted of dividing the anodic and cathodic stimulus phases into a variable number of periods of current delivery alternated with periods of quiescence. Although peak current and total charge did not change, the time course of charge delivery did. As Fig. 14 shows, response sensitivity was greater for "split pulse" waveforms than for uninterrupted pulses. The retention (and even improvement) in sensitivity when the stimulus phases are fragmented suggests that interleaved-pulse stimulation algorithms (e.g., Wilson *et al.*, 1987) are tenable approaches to the problem of avoiding current field summation during simultaneous multichannel stimulation. This very significant finding deserves more study.

We also began studying the ability of electrically stimulated auditory nerve fibers to encode amplitude modulation. We found that fibers did an outstanding job of signaling modulation envelopes. Modulation thresholds, defined as the modulation depth at which phase-locking to the stimulus envelope exceeds a synchronization index of 0.1, were typically 1-2%. This corresponds closely to psychophysical performance of implanted humans (Shannon, unpublished) and strongly suggests that perceptual information about amplitude modulation envelopes is encoded temporally. Representative data, in the form of period histograms and synchronization index (to the fundamental) across modulation depths, are shown in Fig. 15.

Last, we performed a series of studies to obtain input-output functions from auditory nerve fibers stimulated with biphasic pulses in which a temporal gap existed between the anodic and cathodic phases. In all fibers so studied, lengthening the temporal gap produced an improvement in response threshold but no change in rate of response growth or saturation rate. The maximum threshold improvement was typically 2 dB, and the range of gaps over which thresholds improved was 120-150 uS. Temporal gaps >150 uS showed no further improvement in threshold.

Intensity Discrimination. A few fibers were tested on a two-alternative forced-choice intensity discrimination task. The task was identical to that performed in human psychophysics. That is, two pulse trains at different intensities were presented, and, using an adaptive tracking paradigm (Levitt, 1970) that adjusts the intensity of one of the pulse trains from trial to trial, fibers were forced to track pre-selected performance levels. Collection of these tracks allowed us to determine intensity difference limens and construct neural equivalents of psychometric functions. An example is shown in Fig. 16. These data show that the magnitude of the difference limen depends on overall intensity, being higher at lower overall intensities, and that performance improves extraordinarily rapidly as the intensity difference increases. The data obtained from single fibers correlate closely with those obtained from human listeners (Shannon, 1983). This suggests that rate responses of single auditory nerve fibers account fully for perceptual performance, and, unlike theoretical models employed in acoustic work (e.g., Viemeister, 1988), that

combining responses from groups of fibers is not needed to explain behavioral performance.

Responses from Deafened Animals. Responses obtained from animals with long- and short-term deafness were compared with those obtained from animals that possessed normal hearing at the time of implantation. Total deafness was induced in a single treatment by injecting 200 mg/kg kanamycin intramuscularly and following that, two hours later, with an intravenous infusion of 1 mg/ml ethacrynic acid. We monitored auditory brainstem responses (ABRs) during ethacrynic acid administration and stopped when acoustic sensitivity to unfiltered clicks was lost (i.e., when the ABR obtained at 80 dB peak SPL went flat). With this technique we could reliable induce total deafness without causing renal stress or other adverse side effects.

Response thresholds for high-threshold fibers (i.e., those presumably not located near the stimulating electrodes) were lower in deafened animals than in undeafened animals. All other aspects of the response to pulsatile electrical stimuli were similar in deafened and undeafened animals, with two exceptions. First, there was a relative lack of longer-latency (>600 uS) responses in deafened animals. This finding is consistent with degeneration of spiral ganglion cell peripheral processes. And second, in deafened animals fibers forced to respond at high (>200 spikes/S) discharge rates to continuous stimulation often abruptly stopped responding for several seconds, then resumed just as abruptly. The amount of time that fibers ceased responding and the time intervals between periods of response cessation both depended on stimulus intensity. These responses are reminiscent of the "rhythmic" responses observable in the auditory nerves of very immature animals (Walsh and McGee, 1986), and they suggest that membrane potentials of inactive spiral ganglion cells are highly unstable. The cochleas of the deafened animals are currently being evaluated histologically.

Vestibular nerve fibers (identified by regularly occurring spontaneous discharges and an anatomic location in the superior one-third of the cochlear nerve) were easier to excite in deafened animals than in normal-hearing animals. The reason for this is unclear but may be due to the loss of peripheral processes in the spiral ganglion, which in turn can introduce a low-impedance path to the trunk of the cochlear nerve. Once electrical stimulation threshold (>1 mA) was exceeded, responses of presumed vestibular fibers to electrical pulses were indistinguishable from those of auditory fibers.

2. Physiological Studies (van den Honert)

Studies performed in the 3M Biosciences Laboratory over the last 9 years have focused on describing the temporal structure of auditory nerve fiber responses to monopolar and bipolar electrical stimuli, on determining the effects of current field orientation on the spatial extent of the excitatory response, on modeling the effects of current flow in myelinated axons, and on developing novel speech processing schemes for clinical use. These findings are described in van den Honert and Stypulkowski (1984), Stypulkowski and van den Honert (1984), van den Honert and Stypulkowski (1987), and van den Honert (1989). Readers are referred to those publications for further information.

3. Modeling Studies (Finley)

Studies we have conducted over the past 7 years at RTI involve the development of biophysically based models of neural responsiveness to electrical stimulation. The work has focused primarily on understanding how the UCSF cochlear implant system operates. More recently, however, this focus has broadened to include other implant systems by way of emphasizing identification of basic principles and mechanisms active in the electrically stimulated ear. The modeling effort has been expansive and highly integrative. We seek to understand how specific electrode configurations generate electrical fields that influence both single and multiple neurons to produce psychophysical percepts. The full extent of our modeling effort is reflected across Projects II-V of this program project. In the discussion that follows, we will address specifically the responsiveness of a single neuron to electrical stimulation.

The specific aims of work done to date have been to (1) characterize how a single neuron spatially samples the extracellular electrical environment, (2) determine the properties of a neuron that govern its temporal responsiveness, (3) explain electrophysiological data collected from several different laboratories, and (4) establish a set of biophysical models that serve to condense experimental data, create new hypotheses and provide a basis for ultimate optimization of prosthesis systems.

Integrated Field-Neuron Model. We have developed an integrated field-neuron model to couple the fine details of electrical field structures with the full electroanatomy of the cochlea and the physiology of neural elements (Finley and Wilson, 1985). This model allowed us to compute potential gradients along the locus of neural elements using the finite difference method, and it allowed us to calculate the resultant neural response using a variation of the McNeal (1976) model. Examples of these are shown in Fig. 17. This model demonstrated that electrode geometry and placement within scala tympani significantly affected the local extra-cellular field potentials near the target neurons, as is shown in Fig. 18.

Lumped-Element Nonlinear Deterministic Model with Cell Body. We expanded the integrated field-neuron

model to explore the effects on electrical stimulation by the ganglion cell body (Finley, 1989). Fig. 19 summarizes the results from this model. The general finding here is that the presence of the cell body, coupled with extracellular electrical field patterns that may be expected in the cochlea, produces significantly different response properties of spatially segmented nodes of Ranvier that appear as polarity- and level-dependent changes of latency and action potential waveshape. As described earlier, Javel's (1989) physiological data tend to support this prediction.

Results obtained with this preliminary model indicate that the presence of the cell body significantly alters the distribution of sites of excitation along the fiber. The effect clearly depends on stimulus polarity and temporal fine structure, and probably on the magnitude and shape of the extracellular potential profile as well. These findings may help explain the bimodal latency distributions of single units to biphasic pulsatile stimuli described by Javel *et al.* (1987) and van den Honert and Stypulkowski (1987), compound action potential waveshapes obtained in response to monophasic stimuli (Stypulkowski and van den Honert, 1984), and extracellularly recorded waveforms of spiral ganglion action potentials (Robertson, 1984).

4. Modeling Studies (White)

Specific aims of work done at UCSF and North Carolina State over the past 7 years have been to account for the stochastic, noisy behavior of the electrically stimulated auditory neuron, and to determine the effects of variable node width and internal resistance on input-output functions and temporal response properties. The models that have been developed to date, and which will be tested and expanded upon in the studies proposed below, are as follows:

Linear Passive Lumped-Element Neural Model. In this study, we explored the effects of fiber and node dimensions on excitability. Liberman and Oliver's (1984) findings indicate that a 7:1 range of diameters exists in the cat cochlea for nodes peripheral to the cell body, and that a 3:1 range exists for nodes central to the cell body. In addition, the average node diameter of central nodes is about 3.5 times larger than that for peripheral nodes. In one set of simulations we used a simple passive multi-node model like that illustrated in Fig. 21. The membrane resistance (Rm), membrane capacitance (Cm), and internal resistance (Ri) were estimated for each node using Liberman and Oliver's data on fiber diameters and node dimensions. The analysis showed that, for small diameter cochlear afferents, the axonal resistance (Ri) between two adjacent nodes can match or exceed than the transmembrane impedance of the nodes. For small fibers this means that changes in membrane impedance can have a large effect on the voltage developed across the membrane and, therefore, can have a large affect on excitability. In contrast, the voltage developed across nodes in large diameter fibers is relatively insensitive to changing membrane impedance. Because changes in the spectrum of the stimulus change the membrane's impedance, fiber diameter and internode resistance could play an important role in determining a node's sensitivity or insensitivity to such changes.

We determined that the voltage across a node's membrane was directly related to the second spatial derivative of the field in the extracellular medium (Finley *et al.*, 1990). Also, we found that a node's voltage was generally larger if the node was near an abrupt change in impedance (*e.g.*, near a cell-body or near a change in fiber diameter). Because the voltage across a node is a first-order indicator of the node's excitability, the second spatial derivative and impedance discontinuities may be particularly significant variables in determining a node's excitability.

Nonlinear Deterministic Membrane Model. We developed a modified Hodgkin-Huxley (H-H) model with a single homogenous node driven with a current source using one internal and one external electrode. Simulations with this model indicate that membrane impedance and excitability can increase dramatically at low sinusoidal frequencies and at low square-wave frequencies (White, 1984; Tasaki, 1982). The behavior appears to be somewhat analogous to a resonant system, where a previous phase of hyperpolarization can increase the membrane's excitability to the next depolarizing phase of stimulation (see Fig. 22). This may explain the extreme dip observed in thresholds at 100 Hz in some fibers (Hartmann and Klinke, 1990) and also observed in behavioral thresholds in patients and animals (Pfingst, 1982). However, Hartmann and Klinke also found fibers that were relatively insensitive to changes in stimulus spectrum. Our simulations of a multi-node passive model (see previous paragraphs) indicate that larger diameter fibers, in contrast to smaller fibers, will be relatively insensitive to changes in membrane impedance due to changes in stimulus spectrum. Thus Hartmann and Klinke's different fiber response profiles may be the result of large differences that exist in fiber diameters in the cochlea.

Simple Single Node Stochastic Model. Verveen (1962) postulated that neural membrane noise is generated by individual channel activity in the nodal membrane. In nodes with smaller surface areas there are relatively few channels. Therefore, an individual channel's probabalistic activity has a proportionately greater influence on the node's behavior. Verveen determined how the probability of discharge varies with electrical stimulus intensity for a wide range of fibers with different nodal surface areas. For certain stimulus conditions, Verveen found that functions relating discharge probability to stimulus amplitude were described well by integrated Gaussian

functions. Hill's model (Fig. 23) was modified by Verveen so that it would exhibit this simple form of stochastic behavior (see Fig. 24).

Through a series of experiments Verveen found that the slopes of these fiber input-output functions were monotonically increasing functions of nodal surface area. Using Verveen's equation relating surface area to slope and using measured diameters and lengths of nodes of Ranvier of Type I afferent neurons in the cat cochlea (Liberman and Oliver, 1984), we (White *et al.*, 1987) computed the integrated Gaussian input-output functions for the central (Fig. 25) and peripheral (Fig. 26) processes in the cat. We then computed dynamic ranges in dB for each input-output function by determining the stimulus range required to span an 0.1 to 0.9 response probability for the fiber. The predicted dynamic ranges were nearly identical to those directly measured by Javel *et al.* (1987) in the electrically stimulated cat cochlea. When combined with a commonly used behavioral threshold model, this simple stochastic model has proven useful in predicting behavioral temporal integration functions, psychometric functions, and dynamic ranges from psychophysical experiments (see Preliminary Studies in Project V).

Spike Latency Model Based on Neural Conduction. We developed a simple model that predicts spike latency on the basis of estimates of action potential latency through cell segments of variable conduction velocity. In contrast with suggestions (van den Honert and Stypulkowski, 1984) that C responses (Fig. 1) stem from direct excitation of inner hair cells, our model indicates that the time difference between the C and B responses (Fig. 1) may result from an action potential traveling one internodal distance along the very-small-diameter peripheral processes in the cochlea (i.e., 150 microns at approximately 1 meter/sec). The model, if true, suggests that C responses should be observable in recordings from deafened ears.

Stochastic Multi-Node Model. In simulations using a simple stochastic multi-node model (Fig. 27), we found that small nodes generated the majority of initial discharges at low stimulus levels. In contrast, this model predicts that larger nodes generate the majority of activity at higher intensities. This behavior was caused by differences in the slopes of input-output functions predicted by excitation at nodes of widely varying diameter. Verveen's (1962) model is also useful at predicting the temporal dispersion or standard deviation of discharge latencies. Specifically, this model predicts that jitter will be relatively large when small nodes are initially excited and will decrease as intensity increases. These predictions are consistent with Javel's data (see Fig. 7) in that the slopes of the input-output functions for the A and B components co-vary with the standard deviations of the latencies in exactly the manner predicted. Also consistent with the model are van den Honert and Stypulkowski's (1984) findings, which indicate that A responses result from excitation of proximal, large diameter nodes.

Stochastic Multi-Fiber, Multi-Node Model. Using the same multi-node fiber model, we (White, 1986) studied how neural activity was generated by a representative population of model fibers. Model fibers were constructed to represent the wide range of fiber and node dimensions observed by Liberman and Oliver (1984). At the lowest stimulus levels, the smallest diameter fibers carried the majority of neural activity, with the peripheral nodes initially being excited. At higher stimulus levels, the larger diameter fibers and nodes dominated. As before, this pattern of responses resulted from the differences in the slopes of the input-output functions.

D. Experimental Design and Methods

1. Introduction

The description of methods provided here involves more detail than is typically presented in Federal grants. It was done this way for a purpose, which was to state all general physiological and histological methods only once in this application, rather than reiterate the same methods in each project. Physiological techniques described in other projects supplement the methods described here and are applicable only to that project.

2. General Methods

a. Subjects

Single-cell responses of auditory nerve fibers and bushy cells of AVCN will be obtained acutely from young adult cats that exhibit no manifestations of chronic illness or diseases of the external or middle ears. Animals will be purchased from two sources, depending on the way the animal will be studied. Animals used in Projects III and IV will be obtained from the Duke University Division of Laboratory Animal Resources, and animals used in Project V will be obtained from the University of Toronto Research Animal Care Facility. In both cases the animals are purchased from licensed suppliers and housed in the universities' animal care facilities.

Ten cats will be used yearly in Project III, six in Project IV and eight in Project V. Of the animals used in Projects III and IV, approximately half will possess intact hearing prior to implantation, whereas the remainder will be deafened monaurally. Rather than devote an entire experiment to one aspect of a project (*e.g.*, effects of stimulus

frequency, pulse-pair studies, etc.), each animal will be used to study 3-4 different facets of a project. The particular aspects of neural response to be studied will be determined in advance and programmed into our automated data collection system (see Data Acquisition).

b. Pre-Operative Procedures

For 2 days prior to each experiment, all animals will be given tetracycline (500 mg/day) in their drinking water. This is done to retard the development of bacterial infections during the course of physiological recordings, which, depending on the type of study, last 3-6 days.

Normal Hearing Animals. Animals with intact cochleas are used in experiments wherein knowledge of each neuron's CF is required for relating fiber responses to the cochlear locus of stimulation. No special procedures will be performed prior to recording from these animals.

Monaurally Deafened Animals. Monaurally deafened animals are used to produce losses of spiral ganglion cells and peripheral processes, thereby mimicking the situation existing in most humans with cochlear implants. Recordings in these experiments will be taken from bushy cells of AVCN, which retain temporal information to roughly the same extent as the auditory nerve. Stellate and other cells of AVCN will not be studied because their temporal response properties differ from that of the auditory nerve (Rhode *et al.*, 1983; Oertel *et al.*, 1989).

Monaural deafening will be done under sterile conditions as a separate procedure 4-6 months prior to electrophysiological recording. Animals will be anesthetized (see below), the middle ear opened using a posterolateral approach, and 50 ul of 10% neomycin sulfate solution will be injected slowly through the round window. As Pfingst *et al.* (1985), Leake-Jones *et al.* (1980) and others have shown, this procedure effectively destroys inner and outer hair cells in all three cochlear turns, with cells in the basal turns tending to be more affected than the apical turn. Following the neomycin infusion, the loss of acoustic sensitivity will be verified using ABR techniques. When acoustic responsiveness has been lost, the round window will be sealed with a piece of fat, the middle ear will be packed with Gelfoam, and the wound will be closed. The animal will then be returned to its cage, and the wound will be treated with topical antibacterial cream and Xylocaine until it is healed.

c. Intracochlear Electrodes

The electrode array initially used in these studies is the 11-contact experimental electrode described in Project I. These will be fabricated by Dr. Loeb and his co-workers. During the first 3 years of the grant cycle, we will use this electrode exclusively. Starting in the fourth year, Dr. Loeb will provide us with electrodes incorporating advanced designs, among which is the rib-return scheme (see Project I), for use in physiological studies. Although the experimental electrode allows us to vary current field geometry, the extents of the fields produced by this electrode are dissimilar to those produced by rib-return electrodes. Specifically, preliminary modeling work (see Project I) indicates that the rib-return design provides a substantially sharper and more "focused" current field. This in turn predicts that the excited neural population will possess sharper boundaries than the population excited by point-contact electrodes, and that considerable control can be exerted over the site along the spiral ganglion cell at which excitation occurs. Taken together, these differences mean that physiological verification of the predicted behavior of the advanced electrodes is necessary. Accordingly, we will devote the last 1 1/2 - 2 years of the award period to studying neural responses using those electrodes.

d. Surgical Techniques

Anesthesia. At the beginning of the acute electrophysiological experiment the animal is anesthetized to surgical depth with pentobarbital (40 mg/kg, intraperitoneal). Supplemental injections of pentobarbital (10 mg/kg, intramuscular) are administered as necessary throughout the course of the experiment to maintain depth of anesthesia. The need for anesthetic supplements is determined at 2-hour intervals by using a potentially painful pinch to evoke a limb withdrawal reflex. Once anesthetized, animals are never allowed to regain consciousness.

Atropine (0.5 mg daily, intramuscular) is given to reduce fluid secretions in respiratory passages, and dexamethasone (4 mg daily, intramuscular) is administered to retard cerebral edema. Animals receive water and electrolytes (100 ml lactated Ringer's solution) by subcutaneous injection at 24-hour intervals. We have shown that replenishing fluids and electrolytes at regular intervals allows us to obtain good neural records for >4 days in each animal.

Surgery. Surgery immediately preceding data collection is done in the recording chamber under clean but non-sterile conditions. Once an animal has been anesthetized and prepped, it is tracheotomized and mounted in a rigid stereotaxic headholder. Core body temperature is maintained at 39 degrees Celsius by a heating blanket and controller connected to a rectal thermometer. One pinna is removed, leaving a short section of cartilaginous external auditory meatus. The dorsolateral surface of the brainstem is exposed by removing the scalp, reflecting the

temporalis muscle, opening the skull and dura, and aspirating the part of the cerebellum overlying the cochlear nucleus complex. The entire cochlear nucleus is exposed. For experiments involving recordings of auditory nerve fiber responses, surgery continues by wedging bits of cotton between the brainstem and the skull wall to expose the nerve at the point of its exit from the internal auditory meatus.

A custom-built Davies-type chamber is then oriented in the desired plane and cemented to the skull surface. When filled with warm mineral oil and covered with the electrode carrier, the chamber produces a hydraulic seal that reduces brain pulsations and desiccation.

Electrode Insertion. The electrode array is installed by opening the bulla from a posterolateral direction. This approach avoids the eardrum and ossicular chain and provides a good view of the round window. The round window membrane is opened and the array is carefully inserted into scala tympani until resistance is felt. The reason the electrode is not inserted further is that the basal turn of the cat cochlea narrows rapidly at the 8-10 mm point, precluding the possibility of further insertion without damaging the cochlea. Once positioned, cyanoacrylate cement and Dacron mesh are used to fix the electrode in position, and the round window is sealed with a piece of connective tissue. The middle ear is left open. We have shown in non-deafened animals (see Preliminary Studies) that careful electrode insertion does not disturb acoustic sensitivity or neural tuning and response properties, and that adequate acoustic sensitivity is retained for at least 4 days, which is the longest experiment we have conducted to date. Once the electrode has been positioned and secured, individual electrode leads are coupled to a miniature connector, and the impedance of each electrode is tested to ensure electrical continuity.

Earphones. In those experiments where acoustic signals are used to determine neural CF, surgery continues to insert a custom-built earbar into the external auditory meatus. An otoscope is used to position the tip of the earbar within 2 mm of the eardrum, and the cartilaginous meatus is constricted around the earbar speculum with surgical silk, forming a closed acoustic system. This improves earphone response at low frequencies.

e. Acoustic Stimuli and Calibration

In some experiments acoustic stimulation is used to determine neural CF. For this, tones are presented through a Beyer DT-48 dynamic earphone mounted in custom-built shielded enclosures. The earphone is acoustically coupled to the earbar using a piece of flexible tubing. A probe tube is then inserted into the earbar and positioned such that its tip lies flush with the end of the earbar speculum.

A 1/2" B&K condenser microphone and digital signal processing hardware are used in conjunction with the probe tube to perform swept-frequency acoustic calibrations. A software system has been developed to collect and store acoustic calibration data. Earphones are calibrated from 20 Hz to 50 kHz in 20 and 100 Hz steps prior to the beginning of electrophysiological recordings. The calibration tables, which list maximum sound pressure level (SPL, re 20 uPa) available at each frequency, are stored in digital format. They are used with programmable attenuators to set SPL directly during experiments.

Low-distortion acoustic signals (harmonics <-70 dB at all intensities <90 dB SPL, rising to -40 dB at 135 dB SPL) are synthesized and presented using the digital signal system described in Resources and Environment.

f. Electrical Stimuli

Electrical signals delivered to the intracochlear electrodes will be synthesized using our digital signal system and the custom-built voltage-to-current converter and multiplexor listed in the Budget. Software has been developed to generate the desired voltage waveforms, among which are sinusoids, pulse trains, amplitude modulated tones, etc., at a temporal resolution of 5 uS per waveform point. Stimulating waveforms are scaled during synthesis to produce the desired intensity in 0.1-dB steps, up to a maximum of 70 dB peak uA (3.3 peak mA) per phase. The multiplexer provides computer control over the electrodes chosen for current source and sink and allows us to switch stimulating electrodes quickly, under computer control.

The safe limits for application of electrical current are well known. Beyond these limits, electrolysis of the perilymph forms bubbles of hydrogen gas, which in solution is acidic and therefore toxic, and cochlear tissue can be damaged by direct application of high currents. Although gassing is a great concern in clinical implementations of cochlear implants, it is not as critical in acute animal experiments. Nonetheless, care will be taken to ensure that cavitation threshold is not exceeded during our experiments. This consideration is especially important for stimulating electrodes with small surface areas.

g. Data Acquisition

Recording Electrodes. One of two types of recording electrode is used, depending on the experiment being performed. Glass micropipettes filled with 3M KCl are used for experiments involving the auditory nerve. These are fabricated to possess an AC impedance of 20-30 MegOhms at 1000 Hz. Because our electrical stimulus artifact

techniques are quite efficient, there is no need to employ specialized differential recording schemes such as using gold-plated electrodes (van den Honert and Stypulkowski, 1984), balancing circuits (Hartmann *et al.*, 1984), or hybrid techniques (Parkins and Columbo, 1987) to reduce artifact. Parylene- and glass-coated tungsten microelectrodes (Micro-Probe, Inc.) are used for recordings from cochlear nucleus. These are fabricated to possess a tip exposure of about 5 microns and an AC impedance of 5-8 MegOhms at 1000 Hz. We have considerable experience with both electrode types.

The recording electrode is installed in the cover of the Davies chamber and positioned over the brain area of interest. The electrode tip is guided visually to a position over the desired location.

Neuron Isolation. Once placed, the electrode is advanced in 1 micron steps from outside the recording booth using a hydraulic stepping microdrive. The electrode output is amplified and stimulus artifact is rejected (see below). The resulting waveform is displayed on an oscilloscope and made audible through a loudspeaker. Depending on the status of the animal's hearing, either 50-mS bursts of wideband acoustic noise presented at 80 dB SPL or 50-mS trains of biphasic electrical pulses presented at 100 Hz and 60-66 dB uA are used as search stimuli as the electrode is advanced.

Extracellularly recorded activity of single neurons is discriminated on the basis of the positive peak of the action potential, using a template-matching algorithm applied to real-time analog-to-digital records of the electrode output. This provides a more stable estimate of response latency than simple level discrimination. Once the activity of a single neuron has been isolated, spontaneous discharge rate is determined over a 10 S period, and the neuron's CF is determined.

For reasons cited above, recordings in AVCN will be restricted to those from bushy cells. Several investigators have shown that these cells are distinguishable from other cell types in AVCN on the basis of a distinct pre-potential arising from the pre-synaptic end-bulb, as well as by a "primary-like" or "pri-notch" PST histogram shape. We will use both criteria to select cells for study: Only those cells possessing pre-potentials and exhibiting the correct PST histogram shape in response to 50-ms bursts of high-frequency (5 kHz) electrical sinusoids will be included. The purpose of the high-frequency signal is to apply a constant depolarization. "Chopper" cells will exhibit their characteristic "chop" under these conditions (Oertel *et al.*, 1988).

Determination of CF. For experiments in which acoustic sensitivity is retained, a pure-tone tuning curve is taken in 1/24th octave steps using a modification of the algorithm described by Liberman (1978). For experiments in monaurally deafened animals, data are collected from bushy cells in AVCN, and neural CF is determined indirectly by occluding electrically elicited evoked potentials with acoustic stimuli presented contralaterally. The technique is conceptually similar to compound action potential and ABR tuning curves obtained under conditions of simultaneous masking (Dallos and Cheatham, 1976; Mitchell and Fowler, 1980) and the derived-band technique for estimating frequency-specific contributions to ABRs (Don and Eggermont, 1978). The differences are that in this case the masker and probe are presented to different ears, and the probe is an electrical stimulus.

The technique exploits the fact that most neurons in the upper auditory brainstem, and the evoked potentials they produce, are binaurally sensitive (Dobie and Berlin, 1979). A gross (AC impedance <10 kOhms at 1 kHz) electrode is positioned stereotaxically in the inferior colliculus (IC) contralateral to the implanted ear. Because the AVCN is organized tonotopically (Rose *et al.*, 1959) and because single-unit recording electrodes are placed visually, we will already have a rough estimate of neural CF accurate to a resolution of about 1/2 octave. Depending on frequency, this translates into 1-2 mm of distance along the cochlear duct (Liberman, 1982). To determine neural CF more accurately, low-frequency (50 Hz) sinusoidal electrical current is passed through the recording electrode at an intensity sufficient to drive other neurons in the vicinity (25-50 peak uA), and the evoked potential elicited in the contralateral IC is recorded and its amplitude noted. The evoked potential is then partially masked by acoustically stimulating the contralateral, non-deafened ear with pure tones presented continuously at 70 dB SPL, i.e., just below the intensity at which acoustic crossover occurs. The electrically-elicited evoked potential will be maximally occluded or reduced in amplitude when masker frequency coincides with the CF of the electrically stimulated neural region. Plotting evoked potential amplitude as a function of masker frequency allows us to trace out an effective tuning curve.

Importantly, the masking technique should provide positive results regardless of the effect of the contralateral masker at the IC level: Neurons whose responses are excited by contralateral stimuli and inhibited by ipsilateral stimuli (EI cells) will show reduced responses because the masker inhibits the excitatory response to the electrical signal, which is just the effect we need. Likewise, neurons whose responses are excited by stimulation of either ear (EE cells) will also show reduced responses because of occlusion or fatigue produced by the masker. The only cells whose responses do not produce the desired effect are the IE cells, which are not often seen in IC.

Given the fact that our data acquisition software is fully automated and pre-programmable (see Resources and Environment), the process of determining CF should take no longer than 5-6 minutes. This compares favorably with the time required to obtain an acoustic tuning curve.

We have performed a pilot experiment to see if the contralateral masking technique will work as advertised. The pertinent data are shown in Fig. 20. The animal was prepared as described above, except that it possessed

normal hearing in both ears so that we could determine the actual CF of the AVCN region being recorded from. The multi-unit tuning curve obtained from that region is shown at the top of Fig. 20. Evoked-potential amplitudes produced with ipsilateral electrical stimulation through the recording electrode and contralateral acoustic masking are shown at the bottom of Fig. 20. The CFs clearly coincide.

Despite the fact that the masking technique works, the possibility nonetheless exists that, for one reason or another (such as loss of acoustic sensitivity in the non-deafened ear), it may stop working during an experiment. In this case, we have four alternatives. These are listed below in descending order of preference.

1. Record from the ipsilateral LSO. The first alternative is to move the recording electrode to a binaurally sensitive cell group. Two such groups are the contralateral IC, in which neural CFs from deafened ears were successfully estimated by Merzenich *et al.* (1973) and Merzenich and White (1977), and the ipsilateral superior olive (LSO). Of the two, LSO is preferable because effects of anesthesia are less pronounced, because neural responses are usually sustained rather than transient, and because inputs to LSO cells are from the "time-sensitive" rather than the "feature-sensitive" pathway. It is the former pathway which is of primary interest in the studies described here.

LSO can be approached stereotaxically using standard Horsley-Clarke (1908) coordinates. As shown in Berman's (1968) cat atlas, the center of the LSO lies at 4.2 mm lateral, 6.8 mm posterior and 9.5 mm deep from the (0,0,0) reference. CF is then derived from pure-tone acoustic stimulation of the non-deafened ear using the standard tuning curve paradigm. Guinan *et al.* (1972) and Tsuchitani (1977) showed that most LSO neurons are binaurally sensitive and receive inputs from the rostral (anteroventral) cochlear nuclei. They respond primarily with sustained (primary-like or chopper) discharges, and their CFs are identical for stimulation of either ear. In most cases ipsilateral stimulation excites most neurons, whereas contralateral stimulation is usually inhibitory. Inhibitory responses pose no problem for determining CF because a sustained electrically-elicited response can be provided that the acoustic stimulus can diminish, leading to the same CF estimate that would have resulted had the acoustic response been excitatory. The disadvantage of recording from LSO is that temporal response properties of LSO cells may not be directly comparable to those existing in the auditory nerve. Spatial aspects of intracochlear electrical stimulation, however, will still be examinable and will provide us with acceptable measures of response threshold and rate of growth.

2. Use gross estimates of CF based on knowledge of recording location in AVCN. As stated earlier, AVCN is tonotopically organized, and estimates of CF that are based simply on knowledge of the exact recording site are accurate to at least 1/2 octave. We have extensive experience with recording from AVCN, this derived from earlier studies undertaken in developing kittens (Brugge *et al.*, 1975) and in studies involving coding of complex tones. While 1/2-octave resolution is not good enough for some of the studies we propose, it is clearly good enough for others. Also, it is the trends and relative behavior of neural responses along an electrode track that are of value: We don't need to know CF exactly in these cases.

3. Estimate CF by measuring a cell's sensitivity to stimulation of different intracochlear electrodes. In certain cases, CF may be estimated adequately by determining a cell's excitatory threshold as the stimulating current is moved from one radial bipolar electrode pair to another, along the length of the array. This technique will work for cells innervating cochlear loci near the stimulating electrode contacts, but it is likely to fail for cells innervating distant loci. Although this limits the data we would like to collect, the principal needs of the project, which are to determine neural excitability in the region of the stimulating electrodes, will be met.

4. Inject HRP into the auditory nerve. Liberman and Oliver (1984) have shown that horseradish peroxidase can be injected into the auditory nerve and the axons traced back into the cochlea. The two great disadvantages to this technique, however, is that only 3-4 cells with widely separated CFs can be injected per animal, and that the amount of time and effort needed to reconstruct the cochleas is excessive. Dr. Leake (Core B) has considerable experience with anatomic reconstructions of HRP-labeled cells in the spiral ganglion.

Stimulus Presentation and Control. All signals are synthesized digitally using high (100-200 kHz) transfer rates to minimize effects of aliasing, and all signal timing and presentation is done under computer control. Full automation of digitally synthesized signals is a capability our laboratory has possessed for 10 years. Digital synthesis and automated signal presentation maximizes the amount of data obtainable from any given neuron or animal. It also allows us to easily design studies involving the presentation of complicated signal sequences in a predetermined order. Signal parameters are typically pre-selected by the experimenter, and signals are presented sequentially by the computer. The computer automatically varies the selected parameter in the desired direction, and collects, stores and displays data for each trial.

In certain experiments where fixed signal parameters are used repeatedly, as is usually the case in neural population studies, the experimenter can enter desired signal parameters and presentation sequences in a file before the experiment, and execute the commands in that file whenever needed. The computer simply reads the file line by line and takes the desired actions. For example, it is possible to use the automated data collection feature to sequentially determine spontaneous rate, take a tuning curve, set signal parameters (either as absolute values or as values relative to CF or threshold at CF), collect data for a predetermined number of trials, change parameters,

collect more data, etc. All this is accomplished without experimenter intervention.

As signals are being presented, the computer times the occurrence of incoming discharges and updates displays of responsiveness (period histograms, inter-spike interval histograms, post-stimulus time histograms) in real time on a spike-by-spike basis. The computer stores the digitized data on disk and prints a summary at the end of each data collection sequence. Tone parameters are then changed and new sequences initiated, usually for as long as the neuron can be contacted. The availability of real-time displays and data analyses enables us to assess immediately the quality of the data being collected, allows us to reject or repeat trials as necessary, and aids us (based on responses to previous stimuli) in determining the course of study for a given neuron.

Electrophonic Effects and Spontaneous Discharge Rate. In animals with intact cochleas, spontaneously occurring spikes and spikes elicited by electrophonic effects (*i.e.*, as a result of mechanical or electrical stimulation of hair cells) can alter the probabilities of occurrence of spikes elicited by direct electrical excitation. These potentially confounding factors are irrelevant in studies involving the simple determination of sensitivity because (1) knowledge of the exact probability of response is not an issue and (2) electrophonic spikes are easily distinguished from direct-excitation spikes on the basis of latency. However, spontaneous and electrophonic spikes become potentially troublesome in studies involving quantitative measurements of parameters of input-output functions, and in conditions employing long-duration and long-period stimuli. In these cases, we can neutralize the effects of spontaneously occurring spikes by employing brief (single-pulse or single-cycle) stimuli and presenting them only after at least 15 mS have elapsed since the last spike. Multiple studies have shown that 15 mS gives the cell membranes ample time to re-establish a resting state (*e.g.*, Karamanos and Miller, 1988). Also, it is easy to show that electrophonic and spontaneous spikes have no effect on average spike latency and standard deviations of spike occurrence if one takes care (as we routinely do) to confine analyses to a predetermined latency "window". In fact, the only time that electrophonic and spontaneous spikes are truly important is in studies involving the quantitative determination of response probability for long-duration and long-period signals. For long-period signals, we can distinguish electrophonic spikes from direct-excitation spikes by examining spike latencies over a wide range of periods: The trend in latency shift will be very apparent. And in the case of long-duration signals, we will not employ such signals when studying responses of spontaneously active neurons.

Finally, electrophonic spikes originating in cochlear mechanics may arise in recordings from intact ears when the electrical stimulus frequency falls within the response area of the recorded cell. In every case, we know which stimuli will produce electrophonic spikes, and we can avoid using these when necessary. The point being made here is simply that we are familiar with the problems posed by electrophonic and spontaneous spikes, and we are prepared to cope with them in whatever way we can.

Physiological Recordings. In all studies single-cell responses will be recorded over the course of 4 days, or until the animal begins providing poor-quality data. The availability of 5 people to collect data (Javel, van den Honert, Finley, Research Associate, Research Assistant) allows us to work in shifts and collect data around the clock. Regardless of the scientific issue being addressed in a given experiment, every neuron is studied in the same general manner: Once a neuron's responses have been isolated, a measure of spontaneous activity is obtained, and CF is determined. Appropriate signal parameters are then selected, waveforms are synthesized digitally, and stimuli are presented sequentially by the data acquisition computer while displays of neural response are generated and updated in real time. The computer automatically steps parameter values from trial to trial, and the times of occurrence of all spikes are digitized and stored. Once responses to manipulations of one parameter have been studied in sufficient detail, a new parameter is selected for study and the data acquisition sequence repeats. Depending on the number of different cells needed to be studied in a given animal, this process either continues for as long as the neuron can be contacted or until all desired manipulations have been performed, at which time the cell is abandoned.

h. Stimulus Artifact Rejection

Adequate artifact rejection is an important consideration in these experiments because raw stimulus artifact is usually considerably larger than the action potentials being recorded. The techniques we employ for artifact rejection are simpler and require less "tweaking" than those described by others working in implant physiology.

The exact artifact rejection scheme we will employ depends on the stimulus type being used at that moment in time. Rejection schemes for evoked potential work (Project II) are identical to those used in the single-cell work. Artifact rejection is accomplished by a digital signal processing microcomputer (TMS-320C30) with 16-bit A/D and D/A converters. This microcomputer possesses its own memory and DMA connections to the data acquisition computer. It is downloaded by the data acquisition computer with the desired artifact rejection algorithm. During the experiment the microcomputer continuously samples the microelectrode amplifier's output, optionally processes the sample, and re-converts the digital value to an analog voltage, which is tested digitally for the presence of a spike. Sampling occurs at the same transfer rate as the digital waveform synthesizer and is triggered from the same clock. Synchronizing the artifact rejection sampling with the digital waveform synthesizer performs the important task of

eliminating time-delay distortion.

The beginning of an electrical stimulus period is denoted by a brief TTL-compatible pulse sent to a separate input line of the microcomputer. This pulse is generated whenever the low-order bit of digital waveform value is set. The microcomputer monitors the input line and applies the rejection algorithm whenever a voltage level is detected. When no electrical stimulus is present, the microcomputer simply acts as a unity-gain device. That is, its output is exactly the same as the input, and no signal processing is performed.

Short-Duration Pulsatile Stimuli. The artifact rejection algorithm used for short-duration (<400 uS/phase) pulse stimuli is identical for compound action potential (CAP), electrical-evoked auditory brainstem response (EABR), and single-cell recordings. It can be thought of as a variable-duration sample-and-hold or "blanking" operation. The blanking time is specified by the experimenter and sent to the microcomputer by DMA. When the synchronization pulse denoting an electrical stimulus is detected by the microcomputer, blanking duration is read and the voltage output of the recording amplifier is held at the most recently sampled value for the specified amount of time. When the blanking time expires, the microcomputer reverts to the unity-gain operation described above.

Continuous Stimuli. The algorithm used for continuous (sinusoidal) stimuli is a Fourier nulling procedure. In this, one cycle of the stimulus is sampled using a double-buffering approach so that no gaps exist in the digitized record, a forward Fourier transform is performed to create a power spectrum, amplitudes of components corresponding to those in the signal are set to zero, and an inverse Fourier transform is performed to generate the time-domain waveform. Simulations we have performed show that this technique produces excellent (>50 dB) artifact rejection and does not distort spike waveforms. The TMS320C30 chip is fast enough to perform this operation in real time, so long as stimulus period is not exceptionally long.

Long-Duration Pulsatile Stimuli. The remaining artifact rejection technique applies to stimuli with long pulsewidths. It involves the subtraction of a stored artifact template and includes adaptive processes to compensate for fluctuations in artifact amplitude. A spike-free sample of the stimulus artifact is obtained and stored. When a synchronization pulse is received, the microcomputer samples the recording electrode output and subtracts, point for point, the stored artifact sample before re-converting the value to an analog voltage. It also computes an RMS value over the stimulus period, which is provided by DMA. Ideally this value should be close to zero, indicating perfect rejection. If not, a multiplier is computed, the amplitude of the stored artifact sample is scaled in the appropriate direction, and the updated values are used to reject subsequent artifact-containing records. At any time the experimenter can instruct the microcomputer to discard the stored version of the artifact and take a new sample.

i. Morphological Studies

At the conclusion of electrophysiological recordings from animals with deafened ears, the implanted cochlea will be gently perfused with fixative. The temporal bone will be removed (with care taken to leave the implant in place), packed in ice, and sent by overnight courier to Dr. Leake in San Francisco for histological studies to determine (1) the exact position of the implant along the cochlear duct and the relationship of stimulating electrodes to the spiral ganglion, (2) the gross morphology of peripheral spiral ganglion cell processes, and, where needed, (3) detailed information about diameters of nodes of Ranvier. This information is needed for correlating neural responses with modeling work. Further information about histological procedures is given in the description of activities for Core B.

j. Data Analysis

Once an experiment has ended, digitized spike data are available as computer disk files. The files contain stimulus parameters and encoded digital values that allow entire spike trains to be reconstructed to 1-us accuracy and also allow the position of each spike within a stimulus waveform cycle to be calculated to an accuracy of 1 waveform point (typically 5 uS). Subsequent data analysis can proceed in several directions, depending on the specific experiment performed. We employ only those data analyses that are in widespread use in auditory physiology, and we do not anticipate having to develop new analytic procedures.

Over the past nine years we have developed an extensive software library for analysis of single-cell response data. These include routines and programs for mathematical analyses such as least-squares fitting of input-output functions, calculation of synchronization coefficients, Fourier transforms of period and inter-spike interval histograms, and various uni- and multi-variate statistics; programs to re-organize data across trials and print summaries of responses; and programs to plot histograms, input-output functions, tuning curves, Fourier spectra, etc.

The standard sequence of neural data analyses is as follows: Tuning curves, period histograms and post-stimulus time histograms are plotted for all trials. Data from identical trials are merged; and rate-intensity, synchronization-intensity and latency-intensity functions are computed, fitted with nonlinear least-squares procedures, and plotted. Finally, all relevant variables are automatically entered into a relational database that allows us to retrieve any set of information for any subset of stimulus conditions, from any neuron. Following this standard

set of analyses, customized further analyses are designed and implemented. Although the exact nature of a customized analysis cannot be predicted in advance, readers can refer to our published work (Javel *et al.*, 1983; Horst *et al.*, 1986; Javel *et al.*, 1988) for examples of tailored analyses we have undertaken in the past.

3. Experimental Design

a. Introduction

In developing the experimental design of this project, we sought to construct studies such that they provide unambiguous information about ways that variations in stimulus waveforms, current field geometry and anatomic properties define single-cell responses. Also of paramount concern was our desire to design physiological experiments around biophysically based models of intracochlear current spread and neural excitation, and to collect data which allow us to compare neural excitability observed with different electrode designs and in animals with varying degrees of spiral ganglion survival. Preliminary versions of the models to be employed here have been presented in the Preliminary Studies. As work proceeds in Project III, each model will evolve in a standard manner: The model is bench-tested by computer simulation, neural responses to specific stimuli are predicted, the appropriate physiological study is done, the ability of the model to anticipate the physiological data is assessed, and the model is revised accordingly. We feel that only an iterative process incorporating prediction, experimentation and feedback will succeed in meeting our objectives.

Experiments are classified under two general headings. These are *spatial determinants of single-cell response* and *temporal, dynamic and stochastic response properties*. Accordingly, we have defined a 2 x 2 x 2 x 2 matrix of experimental conditions, namely (1) intact *vs.* deafened cochlea, (2) spatial *vs.* temporal stimulus manipulations, (3) 11-contact *vs.* advanced intracochlear electrode design, and (4) auditory nerve *vs.* AVCN recording site. Reviewers should recognize the fact that some of the cells in this matrix require much less data than others. For example, we do not anticipate needing much data from auditory nerve fibers in deafened cochleas or from AVCN cells in intact cochleas. Also, in several cases responses obtained for one cell in the matrix also provide data for other cells. For example, input-output functions taken to study the effects of changing current field geometry also provide latency and temporal dispersion information that tests models of stochastic response behavior. Another consideration is that advanced electrodes will not be avilable until the fourth year of the award period. This effectively halves the number of experimental conditions (from 16 to 8)s we have to consider in the first three years. Thus, the actual scope of the data collection task is not nearly as ambitious as it might seem. A fair estimate is that, on the average, each cell in the matrix must possess good data from at least 60 neurons, or approximately 3 "cat-equivalents" (*i.e.*, the equivalent of studying responses to only one condition in a given cat). Given the manpower and resources available in this project, this goal is eminently achievable in the five years for which funding is requested.

b. Category 1: Spatial Determinants of Single-Cell Response

Rationale. Preliminary modeling work (Finley *et al.*, 1987) indicates that the presence of the spiral ganglion cell body increases the excitability of the closest nodes on the proximal and distal processes of spiral ganglion cells, possibly producing a quantal shift in spike initiation site and response latency as field strength increases and field geometry changes. Similar behavior in acoustic studies of spiral ganglion cell spike waveform (Robertson, 1984) and electrical studies of compound action potential latency (Stypulkowski and van den Honert, 1984) may also relate to cell body effects. Furthermore, stimulus polarity and period may play important roles in determining response threshold and rate of growth (White *et al.*, 1987).

The objectives of the experiments in this category are (1) to obtain detailed quantitative data on neural response threshold and rate of response growth as the geometry of the stimulating field is systematically varied, (2) to determine the conditions under which neurons are excited by transmodiolar and transscalar current flow, (3) to determine the extent of intracochlear current spread and summation for various electrode configurations, and (4) to determine the extent of neural excitation under conditions of partial spiral ganglion degeneration.

Experiment 1.1: Effects of Current Field Orientation. Cats will be implanted with the multiple point-source electrode (Years 1-3), or with an advanced electrode (Years 4-5) developed in Project I. Using the data collection facility in which stimulus parameters can be pre-programmed and automatically presented in the desired sequence, input-output functions will be obtained in 0.4-dB steps for signals consisting of brief (0.05-0.3 ms/phase) biphasic pulses presented at a rate of 50 pulses/S and single cycles of sinusoids of 50-200 Hz frequency presented at 25-100% duty cycle, for monopolar, radial bipolar, longitudinal bipolar, and offset radial field configurations. Data for each condition will be collected until 500 periods have been presented or 300 spikes have been elicited, whichever comes first. The electrodes used to source and sink the current will then be reversed, and

another input-output function will be taken. Following this, a different field-coupling configuration is selected, and the process repeats. If responses to all preselected pairs of electrodes are obtained, data collection will begin anew, either until two iterations of the stimulus set have been performed or until the cell's responses are lost.

Data analyses will focus on the behavior of response parameters (threshold, rate of response growth, and maximum discharge rate) fitted to input-output functions obtained with each electrode configuration. Where possible, iso-response contours will be constructed by plotting the current level required to elicit a given discharge rate as a function of electrode or cell locus. The iso-response data will address questions regarding the spatial extent of the neural response at suprathreshold intensities, in addition to the response at threshold intensities.

Companion modeling work will be done using the integrated field-neuron and finite-element models of extracellular current described in Project II and earlier in this project. Further work with these models will focus on the expected magnitude and spatial extent of extracellular voltage gradients established by the various field configurations, and the correspondence of unit data with model predictions. The studies will proceed in a stepwise progression, beginning with the further development of simple passive membrane neural models. The models will be automatically scaled to auditory neuron dimensions including the cell body segment. Extracellular field profiles for the experimental electrode will be used to scale the extracellular potential sources along the neuronal length. The distribution of currents across and within the neuron will be examined to determine ways in which the neuron samples the external electrical environment. The sensitivity of model parameters on nodal currents (*e.g.*, nodal area, diameters, specific tissue characteristics) will be made by manipulating parameter values by 50% and 200% for each potential profile. Later, this procedure will be repeated for advanced models with more realistic characteristics, and responses will be predicted for pulses with initially different duration and polarity, and for sinusoidal stimuli. The results will be compared with data collected from physiological recordings in which the same neuron has been stimulated with a variety of different stimulus types for different electrode configurations.

Among the hypotheses these manipulations allow us to test are that (1) radial bipolar configurations stimulate spiral ganglion cells by creating local currents along restricted portions of the cell length, (2) monopolar configurations cause current to enter spiral ganglion cells in the vicinity of the cell body and exit as leakage along the central process, (3) that longitudinally oriented bipolar electrodes produce two foci of excitation, one over each electrode; and (4) radial electrode orientations generate neural response patterns in which thresholds are lower in the vicinity of the electrodes but fewer cells are excited (relative to patterns observed for longitudinal or offset radial configuations).

Experiment 1.2: Current Field Summation. Past physiological and psychophysical work has shown that field summation can occur when stimuli are presented simultaneously to two pairs of intracochlear electrodes, and that the net excitation can be greater than that obtained by stimulating either pair alone. While some empirical work on field geometry and channel selectivity has been done (Black and Clark, 1982; van den Honert and Stypulkowski, 1987; Liang, 1988; Spelman, 1989), our understanding of it is still incomplete. Issues that are especially important are the intensity range over which current follows a longitudinal path through the cochlear scalae, the degree of linearity of current field summation, and the effects of peripheral process degeneration and unoccupied habenulae on current paths and magnitudes of cochlear space constants.

Effects of current field summation will be studied using a masking paradigm in which a pulsatile and sinusoidal masker and an identical, in-phase probe are presented simultaneously to different electrode pairs. The masker is fixed in intensity, and an input-output function is taken as probe level is varied. Although this experiment can be set up several ways, depending on the type of data we want to produce, we will focus on only one. In this, the masker and probe signals are always assigned to preselected electrode pairs, and responses from many neurons with different CFs are taken in population-response fashion (*e.g.*, Kim and Molnar, 1977). Prior experience with population studies has shown us that a reasonably complete sample of cells along the entire length of the cochlea can be taken over the course of a 4-5 day experiment. Effects of different field couplings on current summation will be studied systematically. Of particular interest is the documentation of effects at near-threshold masker intensities, to test the hypothesis that facilitation or suppression of the two-signal response occurs in the relative absence of stimulus-elicited discharges (Butikopfer and Lawrence, 1982). Other hypotheses to be tested are that radial electrode configurations produce less current summation

Analysis of these data is very straightforward and focuses on differences between rate-intensity functions and temporal response behavior obtained for the probe in the two conditions, and on threshold and suprathreshold response behavior as a function of cochlear place. Put simply, if variations exist with respect to threshold or rate of response growth for neurons situated between the stimulating electrodes, then field summation or channel interaction exists. The results of this experiment will be used to test the predictions of the field models described in Project II.

c. Category 2: Temporal, Dynamic and Stochastic Response Properties

Rationale. Extensive neural data are currently available for only two stimulus types, namely simple pulses

and sinusoids, and only for recordings in the auditory nerve. Little data exist for other waveshapes, in particular for complex or multi-frequency stimuli. This fact is disappointing because recent data (Wilson, unpublished) show that amplitude-modulated signals with high-frequency carriers produce significantly better speech perception in both single- and multi-channel implant recipients. Also, virtually nothing is known about dynamic or time-varying response properties of electrically stimulated auditory neurons. In this regard, various models of neural excitability suggest that response threshold and rate of growth should differ markedly in neurons with different anatomic features, and that large- and small-node excitation sites should be preferentially stimulated by signals with short and long periods, respectively.

The studies performed in this category address several major issues in electrical stimulus coding. Among these are the effect of waveshape on temporal response properties, the effects of short- and long-term discharge history on neural response behavior, dynamic response properties of electrically stimulated neurons, and stochastic aspects of neural response.

Experiment 2.1: Temporal Processing across the Cochlear Nerve Synapse. The fact that AVCN cells can be contacted for significantly longer periods of time than those of auditory nerve fibers allows us to examine several stimulus manipulations for each cell and relate the responses to one another. Although the auditory nerve provides less ambiguous information about active sites of spike initiation, there is no way we can determine CFs of more than a few auditory nerve fibers in a deafened ear. It is important in the studies named below that we be able to infer aspects of intracochlear electrical fields and neural excitation sites from cochlear nucleus recordings. This is especially true for temporal aspects of neural responses. We already possess a substantial amount of data obtained from auditory nerve fibers in normal and deafened ears in response to pulsatile stimuli presented through a banded (Nucleus/Cochlear) electrode array. To determine the extent to which the cochlear nerve synapse transforms temporal and rate-based responses and to collect physiological data while the experimental electrodes are being fabricated early in the award period, we will collect bushy cell response data from 2 normal hearing cats implanted with banded electrodes already in our possession. Detailed input-output functions (0.4 dB steps) will be obtained in response to short-duration (0.05-0.4 ms/phase) pulses presented to the apicalmost electrode pair. This mimics exactly the conditions for which we have extensive auditory nerve data. Responses will be obtained from 40-60 neurons per animal, and we will sample responses of cells over a wide variety of CFs. Analyses will focus on comparing (1) maximum discharge rates, (2) rates of response growth, (3) temporal dispersion of spikes, and (4) adaptation behavior observed in AVCN with identical data already collected in the auditory nerve. This provides us with the needed database from which we can assess the effects of synaptic processing between the auditory nerve and AVCN. This is the only experiment we will perform with the banded electrode array.

We will employ a stepwise approach to analyzing the AVCN data and comparing it to the auditory nerve findings. If statistical comparisons of raw values for maximum rate, input-output slope, etc., show that these values differ between cochlear nerve and bushy cell responses, we will develop phenomenological models that assume spatial and temporal convergence of inputs and that predict response behavior. Model parameters will be adjusted such that the model's predictions match the physiological data, thereby providing us with firm estimates of the extent to which synaptic processing transforms the auditory nerve input.

Experiment 2.2: Effects of Stimulus Waveform Fine Structure on Temporal Response Patterns. As stated earlier, our understanding of temporal response behavior of electrically stimulated auditory neurons is limited to only two elementary stimulus types. Neural models predict that certain other waveshapes should excite neurons with different anatomic features to different degrees. For example, Hodgkin-Huxley and Frankenhauser-Huxley models both predict that response threshold as a function of stimulus frequency can vary greatly or not at all, depending on the relationship between internal axonal resistance and membrane capacitance.

In this experiment, input-output functions will be obtained sequentially using large (0.8 dB) intensity steps as parameters of pulsatile and sinusoidal waveforms are varied systematically across wide ranges of values. 20-50 stimulus repetitions, each separated in time by 500-1000 mS, will be presented at each intensity. Data will be collected on a stimulus-parameter-by-stimulus-parameter basis: Once a complete set of responses to manipulations of one parameter has been obtained, a new parameter is selected and data collection begins anew.

Stimulus parameters to be manipulated in this experiment are defined by the signal type. For example, for sinusoidal signals the only parameter manipulable is frequency. However, for pulsatile stimuli several parameters are of interest. Among these are pulse rate and aspects of waveform symmetry (e.g., for each phase, trading amplitude for duration while keeping overall charge constant.) We have already begun to study responses under some of these conditions (see Preliminary Studies), but we have only used banded stimulating electrodes and have only investigated the effects of a few stimulus parameters. Another waveform of interest to us from a theoretical point of view is bandpass noise, which may produce reduced and more variable degrees of synchronization, relative to those observed with pulses and higher-frequency sinusoids.

Analyses of these data are very straightforward and will proceed along the same lines we have employed successfully in the past (Javel *et al.*, 1987; Javel, 1989). The data provided by this experiment, in particular the

measures of threshold and dynamic range, form appropriate inputs to the simple and stochastic node models described in the Preliminary Studies. As these models attain further stages of refinement, they will be used to predict how some of the more esoteric signals (*e.g.*, multiphasic pulses) should affect neural excitability and temporal response structure.

Experiment 2.3: Dynamic Response Properties. Stochastic node models (Hill, 1936; Verveen, 1962; White, 1984; Motz and Rattay, 1986) predict very different behaviors in responses containing multiple discharges, depending on the way the model is constructed. For example, Hill's and Verveen's models, which possess no descriptions of refractoriness, are technically applicable only to the first spike elicited. These models are generally poorly developed and cannot account for dynamic or time-varying response properties.

Input-output functions and analyses of temporal response patterns (e.g., period and ISI histograms and their Fourier transforms) will be obtained as the long- and short-term temporal envelopes of stimulus waveforms are systematically varied. Separate studies involving manipulations of pulse rise time, stimulus polarity, and the parameters of amplitude modulated signals (i.e., modulation depth, carrier and modulation frequency, and modulator waveshape) will be conducted. In a related approach to the issue of dynamic response properties, fine-grain analyses of response probability as a function of time will be obtained for stationary pulse trains and sinusoids presented at relatively low (50-100 Hz) frequencies in 200 mS bursts. To negate the influences of electrophonic and spontaneously occurring spikes, these studies will be performed only in deafened animals. Knowledge of CF, while desirable, is not necessary.

Our goal in the modeling work accompanying the physiological studies in Experiment 2.3 is to incorporate sources of refractory behavior into passive and active node models in an attempt to account for neural adaptation and refractory effects. The course these studies will follow is difficult to predict at the present because we lack the needed physiological data. It should be clear that accurate predictions of excitability during a sustained stimulus is an important goal of cochlear implant modeling.

Experiment 2.4: Temporal Integration and Refractory Effects. Effects of neural refractoriness, discharge history and temporal integration will be studied using a forward or non-simultaneous masking paradigm. A complete rate-intensity function for a brief (single-pulse or low-frequency tone burst) signal will be obtained in 0.4 dB steps. In psychophysical terms this is the "probe" signal. Then, the rate-intensity function is repeated for the same stimulus, now in the presence of a fixed-intensity signal, the "masker," that precedes it by a fixed amount of time. To obtain a complete a description as possible, we will collect data for logarithmically-spaced time intervals from 0.25-64 ms, logarithmically-spaced masker durations of 0.1-512 ms, and masker intensities in 1-dB steps between threshold and response saturation.

Data analyses will focus on the behavior of rate-intensity functions obtained for the probe as a function of masker intensity. That is, discharge history effects should be manifested as a reduction in the number of spikes elicited by the probe in the "masked" condition. Where possible, physiological data will be compared with existing psychophysical data in human implantees and the predictions of temporal integration models.

Companion modeling work will focus on predicting how discharge history and refractoriness should influence neural responses derived from active nodes of different cross-sectional diameter. Specifically, the models predict differences in probe threshold for constant-total-charge maskers presented at different frequencies or pulse rates.

Experiment 2.5: Node Dynamics. Stochastic node models make several predictions about neural excitability to simple (pulsatile and sinusoidal) stimuli. Differences in excitability due to anatomic differences in the active nodes of Ranvier should be manifested in threshold, dynamic range, chronaxie, strength-duration curves, temporal dispersion of peaks in period histograms, and response probability at near-threshold intensities. Also, spike initiation sites on the central process of the spiral ganglion cell should produce shorter-latency responses than sites on the peripheral process. Furthermore, passive node models predict differences in rate-intensity function behavior as the size of the active node changes. Specifically, rate-intensity functions for spikes originating at small-diameter nodes (*i.e.*, those corresponding to spike initiation sites on the peripheral process of the spiral ganglion cell) should possess shallower slopes and lower thresholds than functions for spikes originating at large-diameter nodes (*i.e.*, central processes), the standard deviation of the response should vary inversely with node diameter, and the frequency-threshold curves should behave differently. Also, an abrupt shift in spike initiation site from the peripheral to the central process should be manifested as a change in slope of the input-output function, and spikes with exceptionally long latencies should occur when the spike initiation site lies along the very thin, unmyelinated segment of the peripheral process. Finally, sensitivity to signals with greatly varying pulsewidths should be vastly different for small- and large-diameter nodes.

To generate data that provide appropriate inputs to the stochastic node models, we will collect detailed (0.2-dB steps) input-output functions for biphasic pulses presented at 20 pulses/S at intensities that range from 3 dB below to 3 dB above neural response threshold. The parameter will be pulsewidth, which will range in logarithmic increments from 0.05 to 25.6 mS. Care will be taken to obtain a sufficient number of spikes, especially at perithreshold intensities, to clearly resolve details of the temporal response. These studies will primarily be

undertaken in the auditory nerves of cats with intact cochleas to ensure the existence of a large number of spiral ganglion cells with peripheral processes, and less data will be obtained from deafened animals. Effects of spontaneous rate and electrophonic activity will be controlled for as described earlier.

Analyses will focus on strength-duration curves (which should possess different slopes for spikes initiated at different anatomic sites), on response probabilities at low discharge rates, and on parameters fitted to rate-intensity functions. Follow-up anatomic work done in Core B will determine the number of spiral ganglion cells in the recorded CF region that possess peripheral processes, and the morphologic condition of intracellular cell components.

In a related vein pertinent to furthering the modeling studies, anatomic data on fiber size, determinations of internodal spacing and node size will be collected by Dr. Leake to determine if nodes of Ranvier remain on the distal sides of ganglion cells located in cochlear regions for which we will have collected neural response data. Sensitivity studies of the models will be done to determine correspondences between anatomical features and neural responses. If the anatomic data fail to provide us with unambiguous information about the morphology of the spiral ganglion at the desired cochlear loci, we are prepared to perform HRP injections of selected auditory nerve fibers (Liberman, 1982) and identify recorded cells unequivocally. As stated above, Dr. Leake has considerable experience with tracing labeled spiral ganglion cells.

4. Timetable

In the first 3 months of the award period, Experiment 2.1 (synaptic processing) will be completed, and the first group of 5 animals will be deafened monaurally and their spiral ganglia allowed to degenerate partially. When the first experimental electrodes are provided by Project I, responses to spatial current manipulations (Experiment 1.1) will be obtained in the auditory nerve and AVCN of intact animals, then in the deafened animals. Field and node modeling work will occur concurrently. These studies will carry into the beginning of the second year, at which time a second group of 5 animals will be deafened monaurally.

Initial attention in Year 2 will focus on executing the stochastic node studies (Experiment 2.5). These studies will be done in the context of spatial manipulations of current fields, by which time we will already possess extensive data from acutely implanted animals. Then, studies of temporal waveform manipulations on neural response fine structure (Experiments 2.2 and 2.3) will be done in both intact and monaurally deafened ears, and data collection for Experiment 2.5 will be completed.

Research attention in the third year will focus on channel interactions using both simultaneous and non-simultaneous masking techniques (Experiments 1.2 and 2.4), initially in intact ears and later in monaurally deafened ears. These studies will carry into the fourth year, at which time the first advanced electrodes will be emerging from characterization studies in Project I. The remainder of data collection time will be devoted to verifying model predictions pertaining to advanced electrodes. Those studies will be conducted using the same techniques described in Experiments 1.1, 1.2 and 2.5.

E. Human Subjects

Not applicable.

F. Vertebrate Animals

The species used in these studies is the cat. Cats are used because there is a larger physiological and anatomic research literature on auditory experiments with cats than for any other species, and data from the studies described here will be compared with findings described in that literature. Also, equipment in our laboratory has been specifically tailored to electrophysiological experiments in cats.

Cats are purchased from and housed at the Duke University Division of Laboratory Animal Resources, an AALAS-approved facility staffed full-time by trained animal care technicians and veterinarians. We have no specific requirements with regard to strain, age or sex. Our only requirements, in experiments involving animals with intact hearing, are that animals be free from upper respiratory infections at the time experiments are performed, and that they possess clean external ear canals and no evidence of hearing loss.

10 animals will be used in Project III in each of the 5 years of the award period. This number is needed because our protocol calls for data from 2 different kinds of experimental study, 2 different stimulating electrode designs, 2 anatomic states of the cochlea, and 2 physiological recording sites. Each of these will be replicated 3 times, for a total of 2 x 2 x 2 x 2 x 3 = 48 animals. Two additional animals will be used to determine the effects of temporal

processing and spatial summation across the cochlear nerve synapse.

Tetracycline (500 mg/day) is administered for 2 days prior to the experiment to retard bacterial infection. Animals are deeply anesthetized with pentobarbital (40 mg/kg, intraperitoneal) at the beginning of each experiment, atropine (0.5 mg/day) is given to reduce secretions, and dexamethasone (4 mg/day) is administered to minimize edema. Once anesthetized animals are never allowed to regain consciousness over the entire 3-6 day course of the experiment. Depth of anesthesia is tested at two-hour intervals by using a potentially painful pinch to evoke a limb withdrawal reflex. If any reflex activity is observed, supplemental anesthetic (pentobarbital, 10 mg/kg) is administered intramuscularly to restore anesthesia depth to surgical levels. Fluids and electrolytes are replenished daily by subcutaneous injection of 100 ml lactated Ringer's solution.

About 5 animals per year will be deafened by chemical means in one ear 4-6 months before an electrophysiological experiment is performed. Details about the procedures to be followed are provided in the Methods section. The long delay time between deafening and experimentation is needed to allow the spiral ganglion to degenerate partially. During this time animals are held in the Animal Quarters. Previous experience with the deafening procedures to be employed here indicate that the animals tolerate it exceptionally well, and that it has no obvious effect on their personalities or social traits.

At the conclusion of the electrophysiological experiments, anesthetized animals are sacrificed either by barbiturate overdose (500 mg pentobarbital, delivered intracardially), or, in cases where inner ears are to be processed histologically, by intracardiac perfusion with a solution containing a tissue fixative.

G. Consultants/Collaborators

Dr. C. Daniel Geisler of the Depts. of Neurophysiology and Electrical Engineering at the University of Wisconsin-Madison, has agreed to serve as a consultant on this project. Dr. Geisler is a recognized authority on auditory stimulus coding, math models of single-cell and cochlear mechanical response, and cochlear electroanatomy. He will spend three days yearly critically reviewing our findings and helping us plan upcoming work. He will also review manuscripts to be submitted for publication. A letter of agreement from Dr. Geisler and a biographical sketch are included in the Appendix.

H. Consortium/Contractual Arrangements

This project will involve a consortium that includes Duke University, Research Triangle Institute, North Carolina State University, and, indirectly, the University of California - San Francisco. Details about consortium/contractual arrangements are given in the Introduction. Administration of funds and procedures for communication among investigators are described in the introduction. Responsibilities of the investigators are described in the budget justification for Project III.

I. Literature Cited

Berman, A.L. (1968) *The Brain Stem of the Cat: A Cytoarchitectonic Atlas with Stereotaxic Coordinates* (Madison, WI: Univ. of Wisconsin Press).

Black, R.C., and Clark, G.M. (1980) Differential electrical excitation of the auditory nerve. J. Acoust. Soc. Am. 67, 868-874.

Brugge, J.F., Javel, E., and Kitzes, L.M. (1978) Signs of functional maturation of peripheral auditory system in discharge patterns of neurons in anteroventral cochlear nucleus of the kitten. J. Neurophysiol. 41, 1557-1579.

Clopton, B.M., and Glass, I. (1984) Unit responses at cochlear nucleus to electrical stimulation through a cochlear prosthesis. Hearing Res. 14, 1-11.

Clopton, B.M., Wiler, J.A., and Backoff, P.M. (1990) Neural processing of complex electric and acoustic stimuli. In J.M. Miller and F.A. Spelman (eds.), *Models of the Electrically Stimulated Cochlea* (New York: Springer-Verlag), pp. 223-243.

Dallos, P., and Cheatham, M.A. (1976) Compound action potential tuning curves. J. Acoust. Soc. Am. 59, 591-597.

Dobie, R.A., and Berlin, C.I. (1979) Binaural interaction in brainstem evoked responses. Arch. Otolaryngol. 105, 391-198.

Don, M., and Eggermont, J.J. (1978) Analysis of the click-evoked brainstem potentials in man using high-pass noise masking. J. Acoust. Soc. Am. 63, 1084-1092.

Dynes, S.B.C., and Delgutte, B. (1989) Phase locking of auditory nerve fiber response to electric sinusoidal stimulation of the cochlea. Abst. Assn. Res. Otolaryngol. 12, 269.

Finley, C.C., and Wilson, B.S. (1985) An integrated field-neuron model of electrical stimulation by intracochlear scala tympani electrodes. Abst. Assn. Res. Otolaryngol. 8, 105-106.

Finley, C.C., Wilson, B.J., and White, M.W. (1987) A finite-element model of bipolar field patterns in the electrically stimulated cochlea -- A two dimensional approximation. In *Proceedings of the 9th Annual Conference on Engineering in Medicine and Biology* (IEEE Press), pp. 1901-1903.

Finley, C.C., Wilson, B.S., and White, M.W. (1990) Models of neural responsiveness to electrical stimulation. In J.M. Miller and F.A. Spelman (eds.), *Models of the Electrically Stimulated Cochlea* (New York: Springer-Verlag), pp. 55-93.

Glass, I. (1983) Tuning characteristics of cochlear nucleus units in response to electrical stimulation of the cochlea. Hear. Res. 12, 223-237.

Glass, I. (1985) Responses of cochlear nucleus units to electrical stimulation through a cochlear prosthesis: Channel interaction. Hear. Res. 17, 115-126.

Guinan, J.J., Guinan, S.S., and Norris, B.E. (1972) Single auditory units in the superior olivary complex. I. Responses to sound and classifications based on physiological properties. Int. J. Neurosci. 4, 101-120.

Hartmann, R., Topp, G., and Klinke, R. (1984) Electrical stimulation of the cat cochlea: Discharge pattern of single auditory fibers. Adv. Audiol. 1, 18-29.

Hartmann, R., and Klinke, R. (1990) Response characteristics of nerve fibers to patterned electrical stimulation. In J.M. Miller and F.A. Spelman (eds.), *Models of the Electrically Stimulated Cochlea* (New York: Springer-Verlag), pp. 135-159.

Hill, A.V. (1936) Excitation and accomodation in nerve. Proc. Royal Soc. 119, 305-355.

Hodgkin, A.L., and Huxley, A.F. (1945) Resting and action potentials in single nerve fibres. J. Physiol. (London) 104, 176-188.

van den Honert, C. (1990) Reproducing auditory nerve temporal patterns with sharply resonant filters. In J.M. Miller and F.A. Spelman (eds.), *Models of the Electrically Stimulated Cochlea* (New York: Springer-Verlag), pp. 115-131.

van den Honert, C., and Stypulkowski, P.H. (1984) Physiological properties of the electrically stimulated auditory nerve. II. Single fiber recordings. Hear. Res. 14, 225-243.

van den Honert, C., and Stypulkowski, P.H. (1987) Temporal response patterns of single auditory nerve fibers elicited by periodic electrical stimuli. Hearing Res. 29, 207-222.

Horsley, V., and Clarke, R.H. (1908) The structure and function of the cerebellum examined by a new method. Brain 31, 45-124.

Horst, J.W., Javel, E., and Farley, G.R. (1986) Coding of spectral fine structure in the auditory nerve. I. Fourier analysis of period and interspike interval histograms. J. Acoust. Soc. Am. 79, 398-416.

Javel, E., McGee, J., Walsh, E.J., Farley, G.R., and Gorga, M.P. (1983) Suppression of auditory nerve responses. II. Suppression threshold and growth, iso-suppression contours. J. Acoust. Soc. Am. 74, 801-813.

Javel, E., Tong, Y.C., Shepherd, R.K., and Clark, G.M. (1987) Responses of cat auditory nerve fibers to biphasic electrical current pulses. Ann. Otol. Rhinol. Laryngol. 96, Suppl. 128, 26-30.

Javel, E. (1990) Acoustic and electrical encoding of temporal information. In J.M. Miller and F.A. Spelman (eds.), *Models of the Electrically Stimulated Cochlea* (New York: Springer-Verlag), pp. 247-292.

Karamanos, N., and Miller, M.I. (1988) A new method for estimating stimulus and refractory related functions from auditory-nerve discharges. In H. Duifhuis, J.W. Horst and H.P. Wit (eds.), *Basic Issues in Hearing* (London: Academic), pp. 185-193.

Kim, D.O., and Molnar, C.E. (1979) A population study of cochlear nerve fibers: Comparison of spatial distributions of average-rate and phse-locking measures of responses to single tones. J. Neurophysiol. 42, 16-30.

Leake, P.A., and Hradek, G.T. (1988) Cochlear pathology of long term neomycin induced deafness in cats. Hear. Res. 33, 11-34.

Leake-Jones, P.A., Vivion, M.C., O'Reilly, B.F., and Merzenich, M.M. (1982) Deaf animal models for studies of a multichannel cochlear prosthesis. Hear. Res. 8, 225-246.

Levitt, H. (1971) Transformed up-down methods in psychoacoustics. J. Acoust. Soc. Am. 49, 467-477.

Liang, D.H.-C. (1988) *The Nerve-Electrode Interface in the Auditory Prosthesis*. Doctoral Thesis, Stanford Univ.

Liberman, M.C. (1978) Auditory-nerve response from cats raised in a low-noise chamber. J. Acoust. Soc. Am. 63, 442-455.

Liberman, M.C. (1982) The cochlear frequency map for the cat: Labeling auditory-nerve fibers of known characteristic frequency. J. Acoust. Soc. Am. 72, 1441-1449.

Liberman, M.C., and Oliver, M.E. (1984) Morphometry of intracellularly labeled neurons of the auditory nerve: Correlations with functional properties. J. Comp. Neurol. 223, 163-176.

McNeal, D.R. (1976) Analysis of a model for excitation of myelinated nerve. IEEE Trans. Biomed. Eng. 23, 329-337.

Merzenich, M.M., Michelson, R.P., Pettit, C.R., Schindler, R.A., and Reid, M. (1973) Neural encoding of sound

sensation evoked by electrical stimulation of the acoustic nerve. Ann. Otol. Rhinol. Laryngol. 82, 486-503.
Merzenich, M.M., and White, M.W. (1977) Cochlear prosthesis: The interface problem. In F.T. Hambrecht and J.B. Reswich (eds.), *Functional Electrical Stimulation* (New York: M. Dekker), pp. 321-340.
Mitchell, C., and Fowler, C. (1980) Tuning curves of cochlear and brainstem responses in the guinea pig. J. Acoust. Soc. Am. 68, 896-900.
Motz, H., and Rattay, F. (1986) A study of the appalication of the Hodgkin-Huxley and the Frankenhaeuser-Huxley model for electrostimulation of the acoustic nerve. Neurosci. 18, 699-712.
Moxon, E.L. (1971) *Neural and Mechanical Responses to Electric Stimulation of the Cat's Inner Ear.* Doctoral thesis, Mass. Inst. Technol.
Oertel, D. (1985) Use of brain slices in the study of the auditory system: Spatial and temporal summation of synaptic inputs in cells in the anteroventral cochlear nucleus of the mouse. J. Acoust. Soc. Am. 78, 328-333.
Oertel, D., Wu, S.H., and Hirsch, J.A. (1988) Electrical characteristics of cells and neuronal circuitry in the cochlear nuclei studied with intracellular recordings from brain slices. In: G.M. Edelman, W.E. Gall and W.M. Cowan (eds.), *Auditory Function: Neurobiological Bases of Hearing* (New York: Wiley), pp. 313-336.
Parkins, C.W., and Columbo, J. (1987) Auditory-nerve single-neuron thresholds to electrical stimulation from scala tympani electrodes. Hear. Res. 31, 267-286.
Pfingst, B.E. (1990) Psychophysical constraints on biophysical/neural models of threshold. In J.M. Miller and F.A. Spelman (eds.), *Models of the Electrically Stimulated Cochlea* (New York: Springer-Verlag), pp. 161-183.
Pfingst, B.E., Glass, I., Spelman, F.A., and Sutton, D. (1985) Psychophysical studies of cochlear implants in monkeys: Clinical implications. In R.A. Schindler and M.M. Merzenich (eds.), *Cochlear Implants* (New York: Raven Press), pp. 305-321.
Pfingst, B.E., Sutton, D., Miller, J.M., and Bohne, B.A. (1981) Cochlear implants: Relation of psychophysical measures to histological findings. Acta Otolaryngol. 92, 1-13.
Pfingst, B.E., and Sutton, D. (1983) Relation of cochlear implant function to histopathology in monkeys. Ann. N.Y. Acad. Sci. 405, 224-239.
Rhode, W.S., Oertel, D., and Smith, P.H. (1983a) Physiological response properties of cells labeled intracellularly with horseradish peroxidase in cat ventral cochlear nucleus. J. Comp. Neurol. 213, 448-463.
Rhode, W.S., Smith, P.H., and Oertel, D. (1983b) Physiological response properties of cells labeled intracellularly with horseradish peroxidase in cat dorsal cochlear nucleus. J. Comp. Neurol. 213, 426-447.
Robertson, D. (1984) Horseradish peroxidase injection of physiologically characterized afferent and efferent neurones in the guinea pig spiral ganglion. Hear. Res. 15, 113-122.
Rose, J.E., Galambos, R., and Hughes, J.R. (1959) Microelectrode studies of the cochlear nuclei of the cat. Bull. Johns Hopkins Hosp. 104, 211-251.
Shannon, R.V. (1983) Multichannel electrical stimulation of the auditory nerve in man. I. Basic psychophysics. Hearing Res. 11, 157-189.
Shepherd, R.K., Clark, G.M., Pyman, B.C., Webb, R.L., Murray, M.T., and Houghton, M.E. (1985) Histopathology following electrode insertion and chronic electrical stimulation. In R.A. Schindler and M.M. Merzenich (eds.), *Cochlear Implants* (New York: Raven Press), pp. 65-81.
Simmons, F.B. (1966) Electrical stimulation of the auditory nerve in man. Arch. Otolaryngol. 84, 2-54.
Spelman, F.A. (1989) Models of current flow. In J.M. Miller and F.A. Spelman (eds.), *Models of the Electrically Stimulated Cochlea* (New York: Springer-Verlag), pp. 35-51.
Stypulkowski, P.J., and van den Honert, C. (1984) Physiological properties of the electrically stimulated auditory nerve. I. Compound action potential recordings. Hear. Res. 14, 205-224.
Tasaki, I. (1982) *Physiology and Electrochemistry of Nerve Fibers* (New York: Academic).
Tsuchitani, C. (1977) Functional organization of lateral cell groups of the cat superior olivary complex. J. Neurophysiol. 40, 296-318.
Verveen, A.A. (1962) Axon diameter and fluctuation in excitability. Acta Morphol. Neerlando-Scand. 5, 79-85.
Viemeister, N.F. (1988) Psychophysical aspects of auditory intensity coding. In G.M. Edelman, W.E. Gall, and W.M. Cowan (eds.), Auditory Function (New York: Wiley), pp. 213-241.
Walsh, E.J., and McGee, J. (1986) The development of function in the auditory periphery. In R.A. Altschuler, R.P. Bobbin, and D.W. Hoffman (eds.), Neurobiology of Hearing: The Cochlea (New York: Raven), pp. 247-270.
White, M.W. (1984) Psychophysical and neurophysiological considerations in the design of a cochlear prosthesis. Audiol. Ital. 1, 77-117.
White, M.W. (1986) Stochastic models of cochlear neural excitation, presented at the *Satellite Symposium on Hearing of the International Union of Physiological Societies*, San Francisco.
White, M.W., Finley, C.C., and Wilson, B.S. (1987) Electrical stimulation of the auditory nerve: Stochastic response characteristics. IEEE / 9th Annual Conference on the Engineering in Medicine and Biology Society, pp. 1906-1907.
Wilson, B.S., Finley, C.C., Lawson, D.T., and Wolford, R.D. (1988) Speech processors for cochlear prostheses. Proc.

IEEE 76, 1143-1154.

Young, E.D., Shofner, W.P., White, J.A., Robert, J.-M., and Voigt, H.F. (1988) Response properties of cochlear nucleus neurons in relationship to physiological mechanisms. In: G.M. Edelman, W.E. Gall and W.M. Cowan (eds.), *Auditory Function: Neurobiological Bases of Hearing* (New York: Wiley), pp. 277-312.

Young, E.D., and Brownell, W.E. (1976) Responses to tones and noise of single cells in dorsal cochlear nucleus of unanesthetized cats. J. Neurophysiol. 39, 282-300.

Young, E.D., and Voigt, H.F. (1982) Response properties of type II and type III units in the dorsal cochlear nucleus. Hear. Res. 6, 153-169.

Figures for Project III

Figure 1

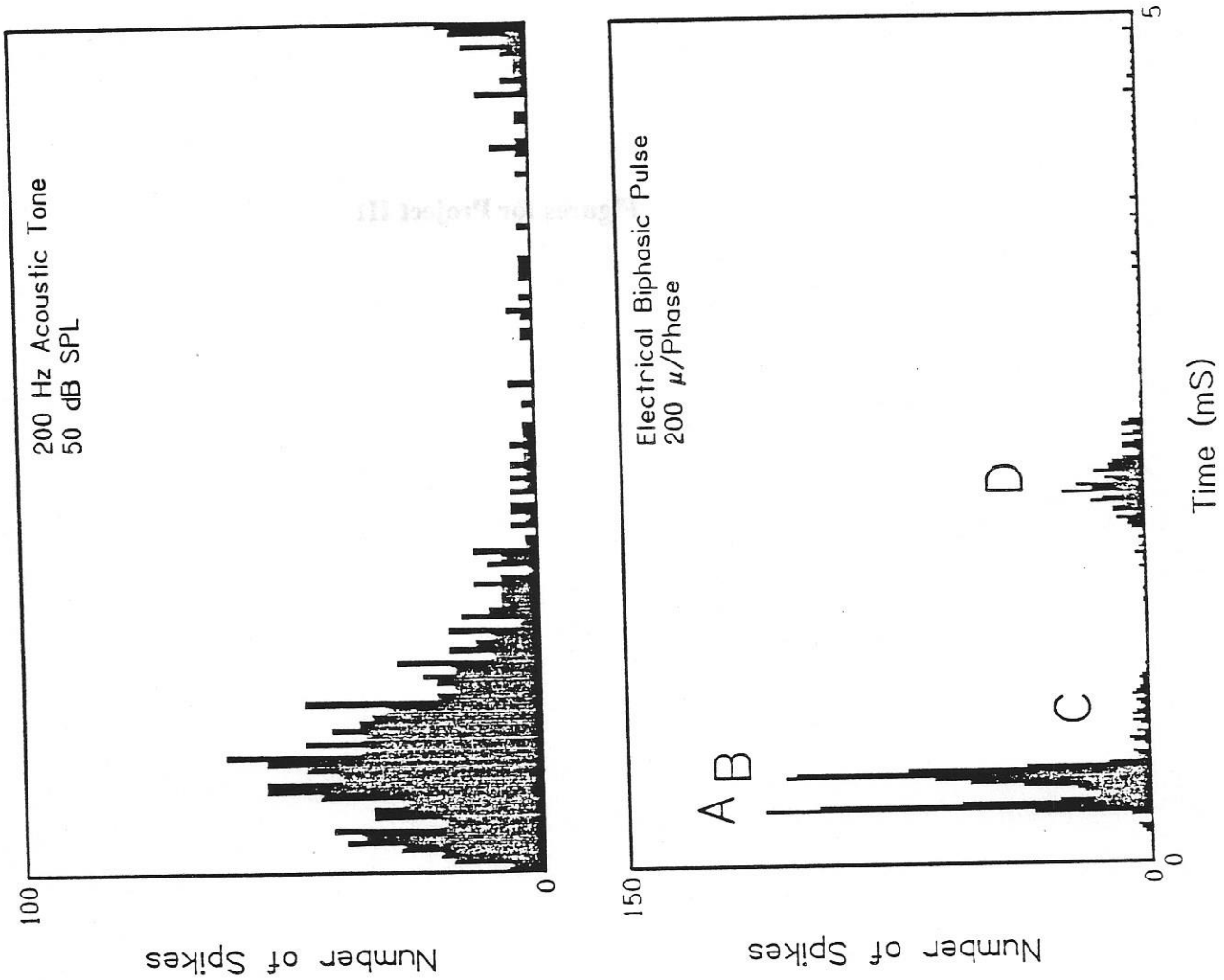
200 Hz Acoustic Tone
50 dB SPL
100
0
Number of Spikes
Electrical Biphasic Pulse
200 μ/Phase
A
B
C
D
150
0
0
5
Number of Spikes
Time (mS)

Neuron 85-E03-3 (100 μsec/phase, 400 pulses/sec)

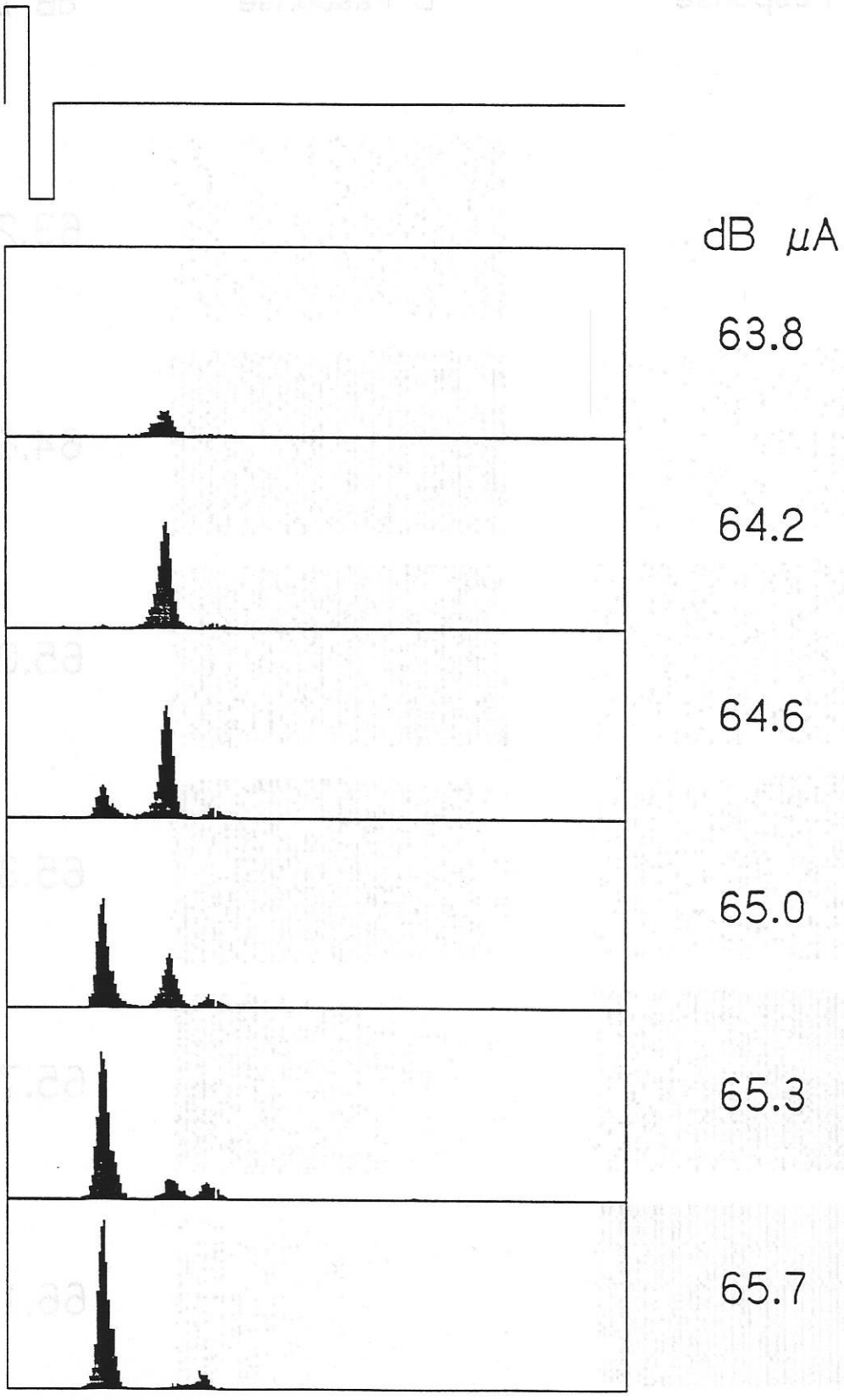

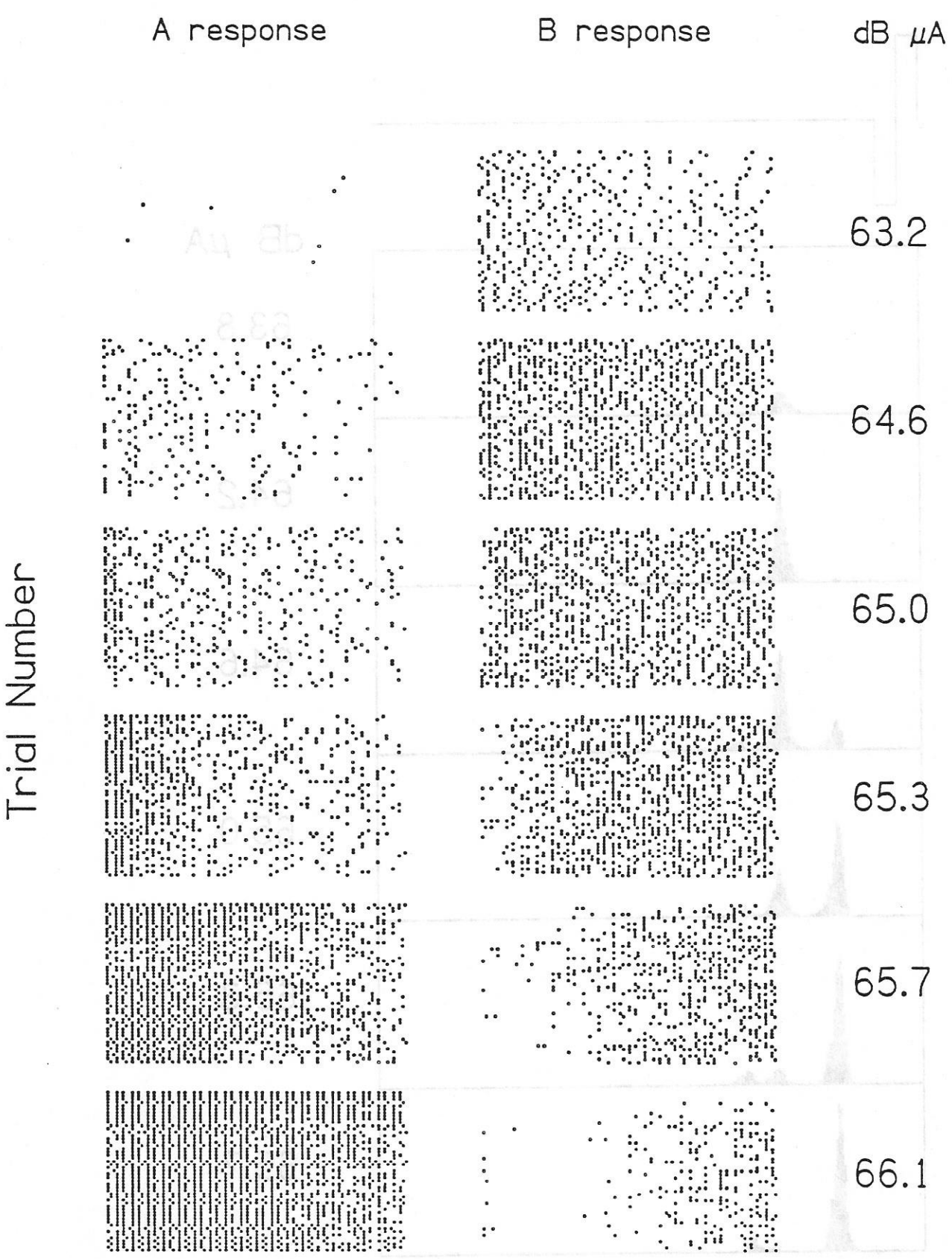
100 μS/Phase 400 Pulses/S Initially Positive
A response
B response
dB μA
63.2
64.6
65.0
65.3
65.7
66.1
Trial Number

Figure 4

Neuron 85-E03-29
Width = 100 μS Rate = 100/S

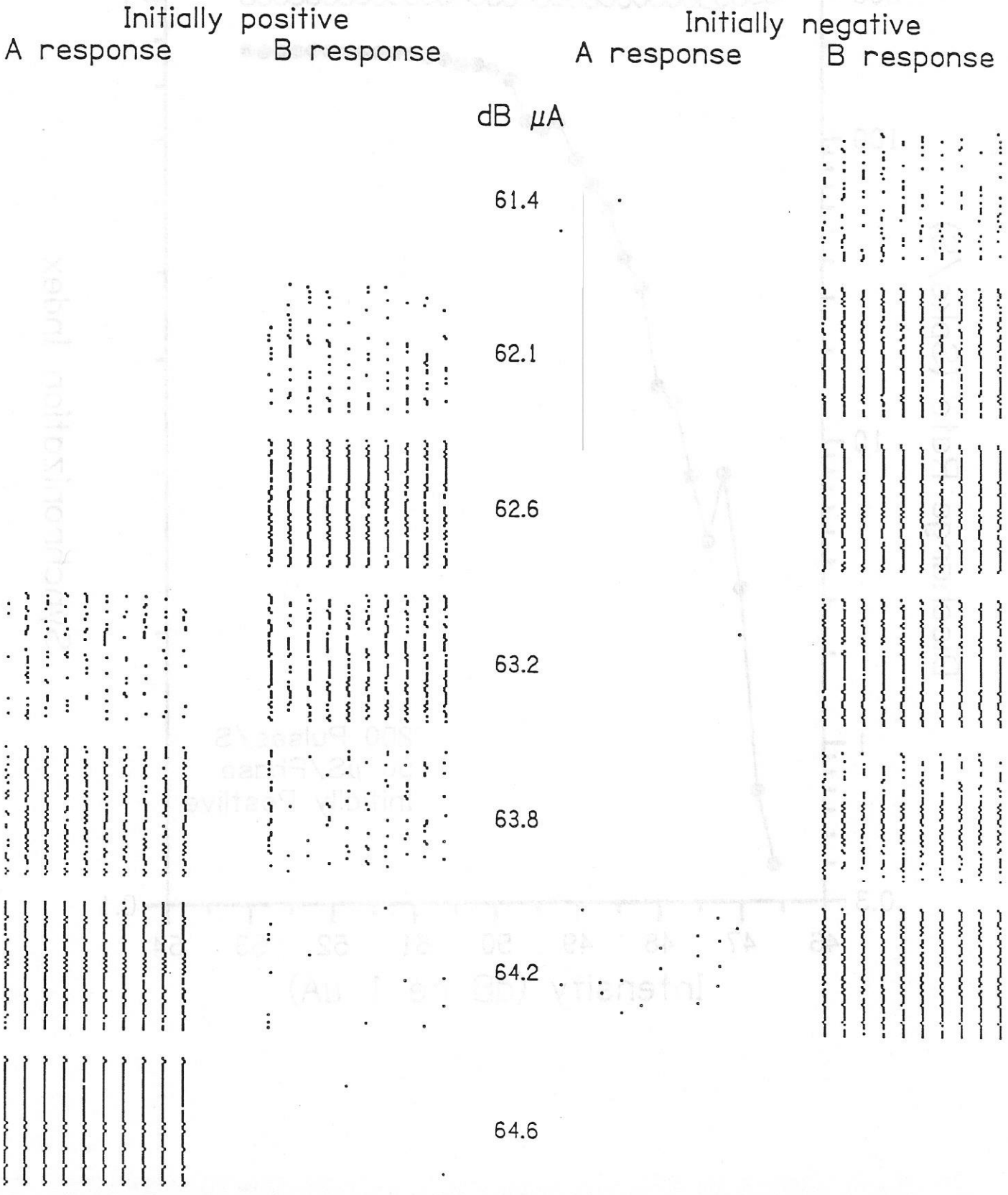

Figure 5

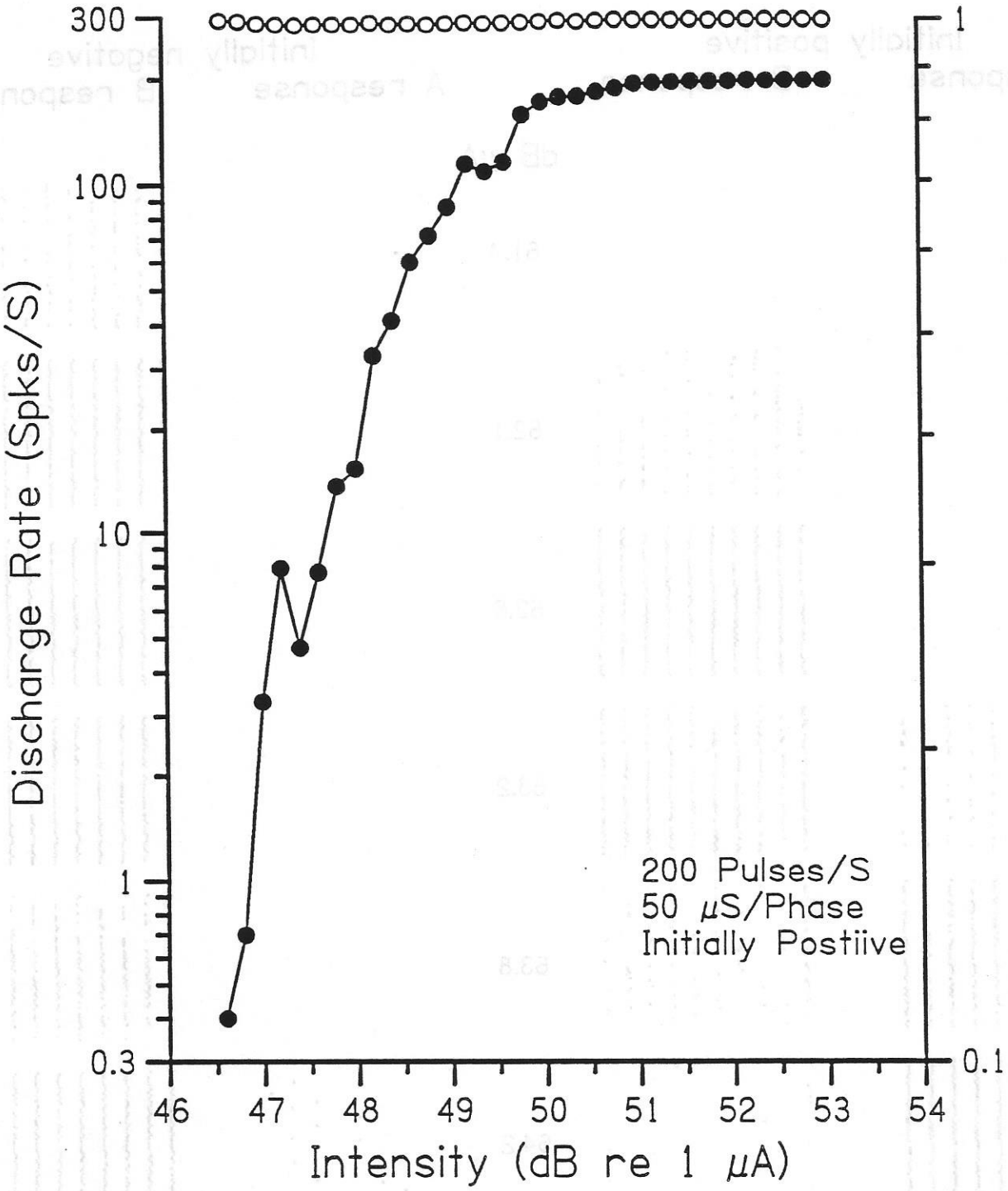
300
100
10
1
0.3
1
0.1
Discharge Rate (Spks/S)
Synchronization Index
200 Pulses/S
50 μS/Phase
Initially Postiive
46
47
48
49
50
51
52
53
54
Intensity (dB re 1 μA)

Figure 6

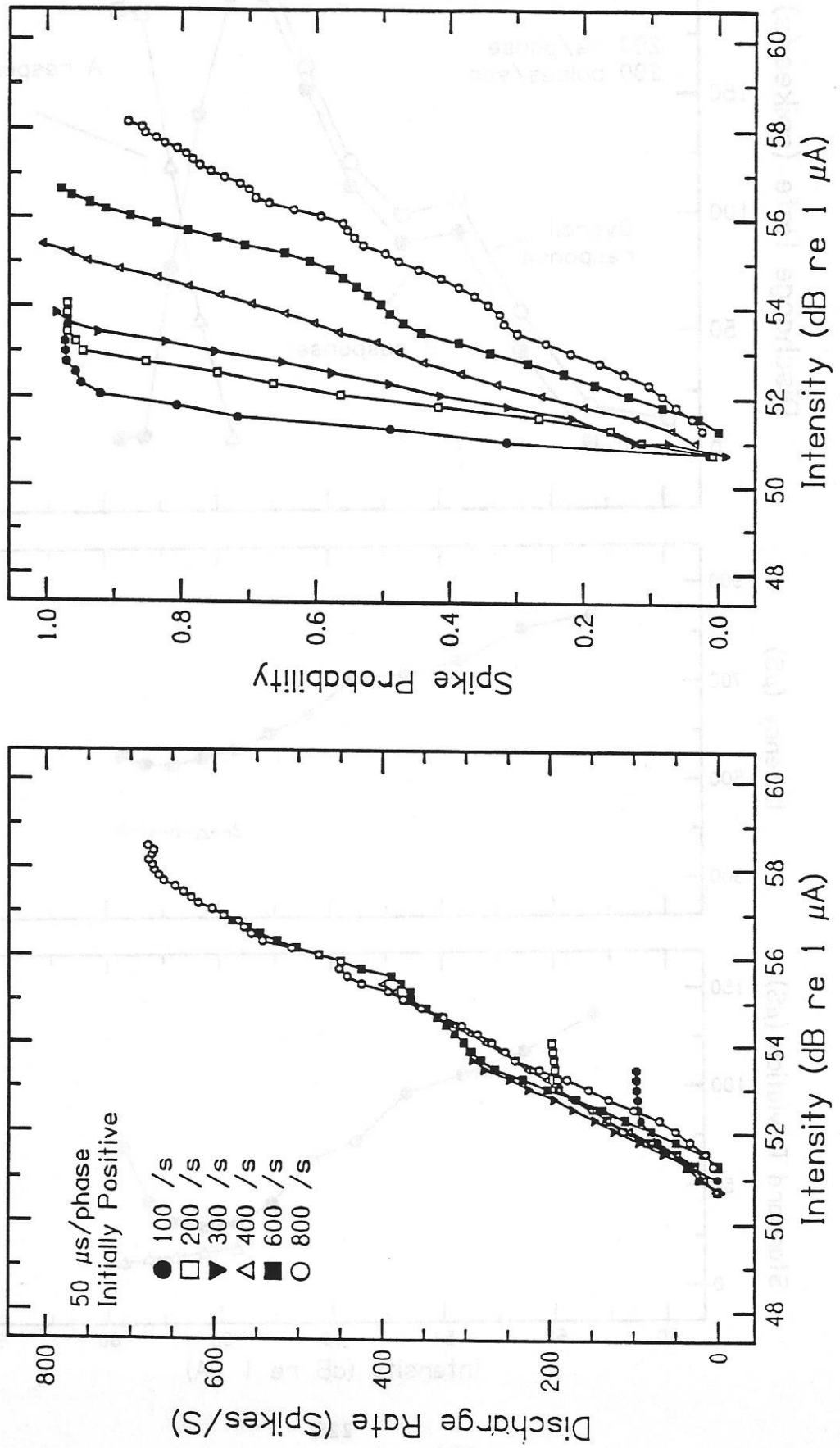
Spike Probability
1.0
0.8
0.6
0.4
0.2
0.0
48
50
52
54
56
58
60
Intensity (dB re 1 μA)
Discharge Rate (Spikes/S)
800
600
400
200
0
50 μs/phase
Initially Positive
● 100 /s
□ 200 /s
▶ 300 /s
△ 400 /s
■ 600 /s
○ 800 /s
48
50
52
54
56
58
60
Intensity (dB re 1 μA)

Figure 7

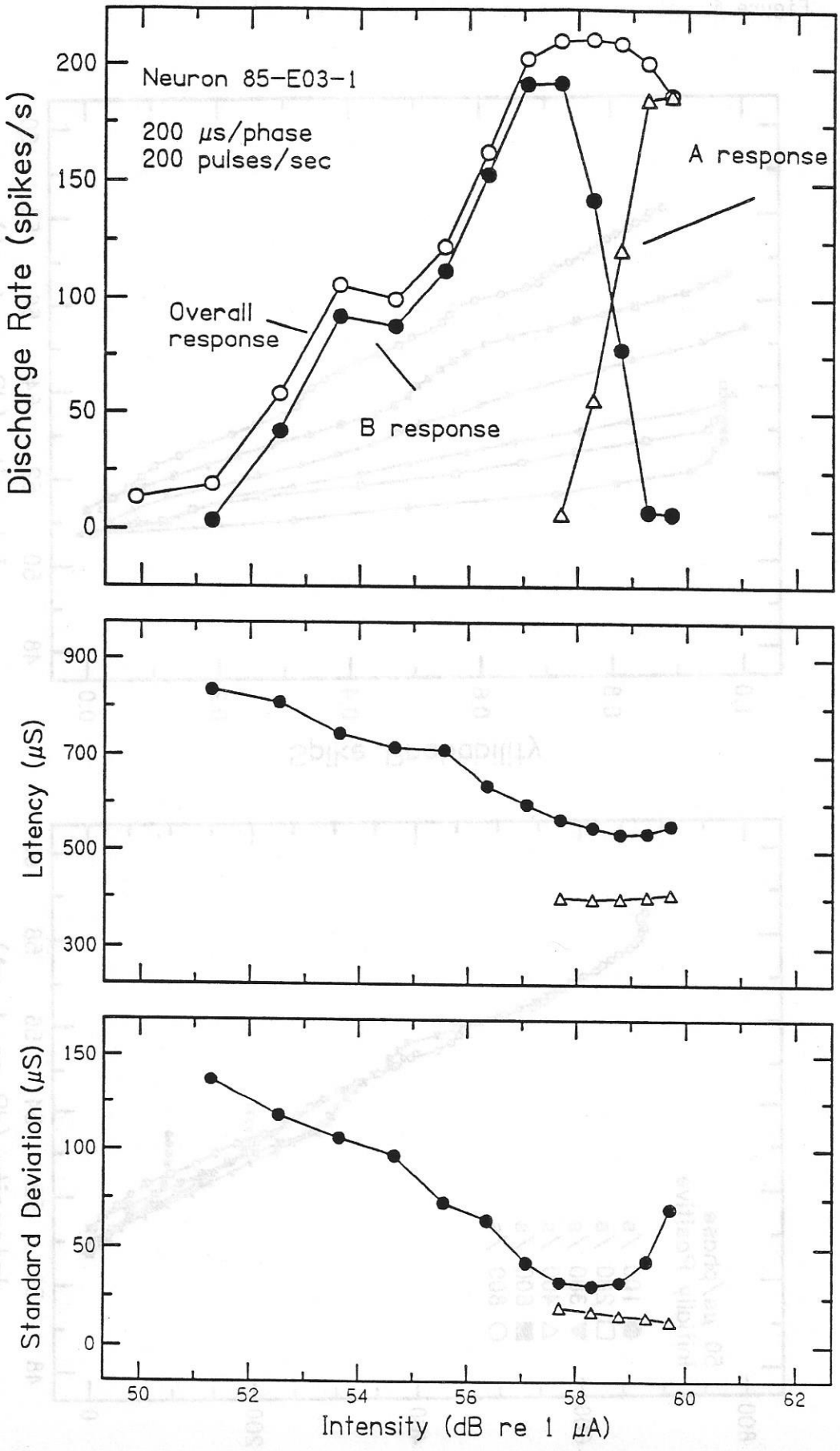
Neuron 85-E03-1
200 μs/phase
200 pulses/sec
A response
Overall response
B response
Discharge Rate (spikes/s)
200
150
100
50
0
Latency (μS)
900
700
500
300
Standard Deviation (μS)
150
100
50
0
50
52
54
56
58
60
62
Intensity (dB re 1 μA)

Figure 8

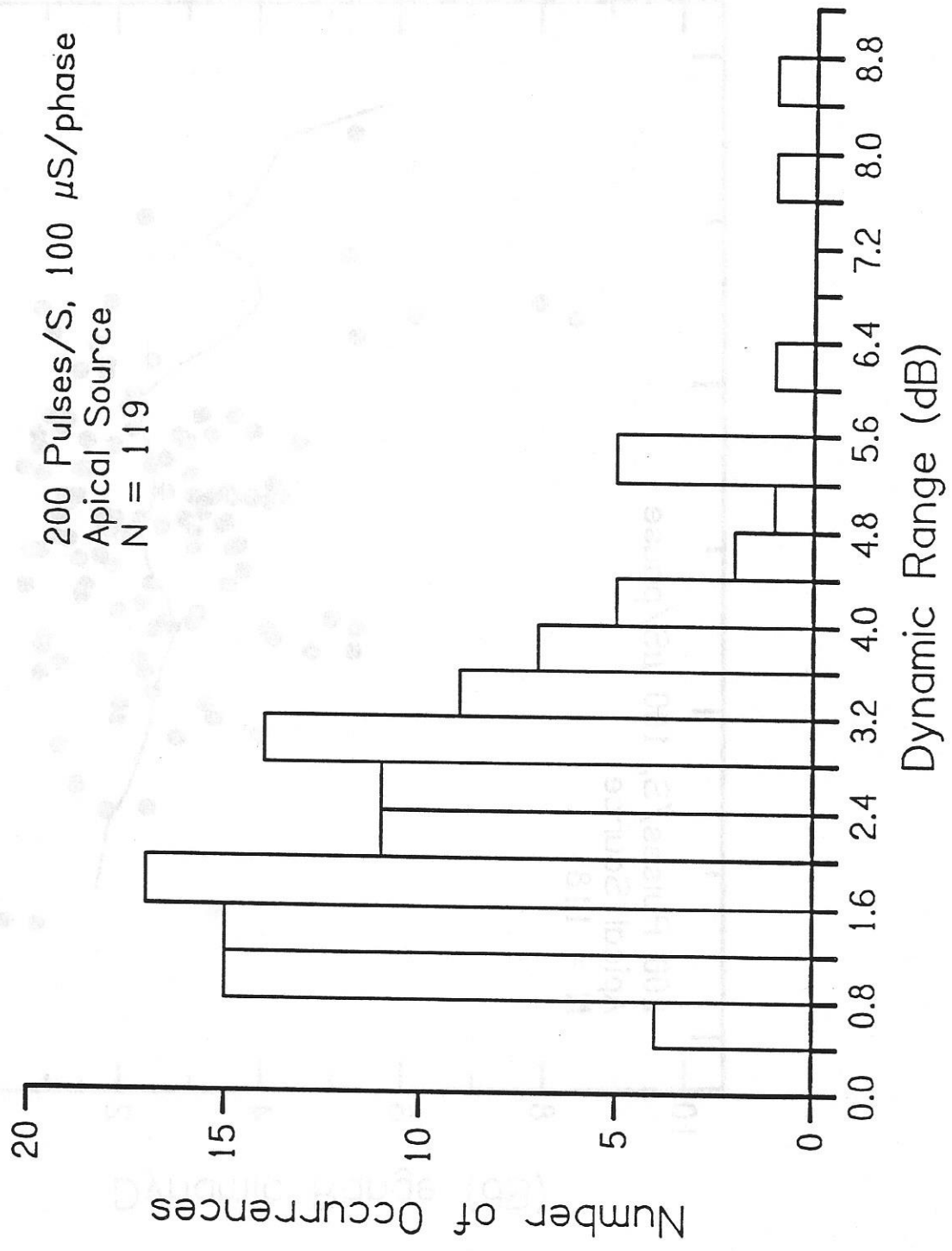
200 Pulses/S, 100 μS/phase
Apical Source
N = 119
Number of Occurrences
0
5
10
15
20
0.0
0.8
1.6
2.4
3.2
4.0
4.8
5.6
6.4
7.2
8.0
8.8
Dynamic Range (dB)

Figure 9

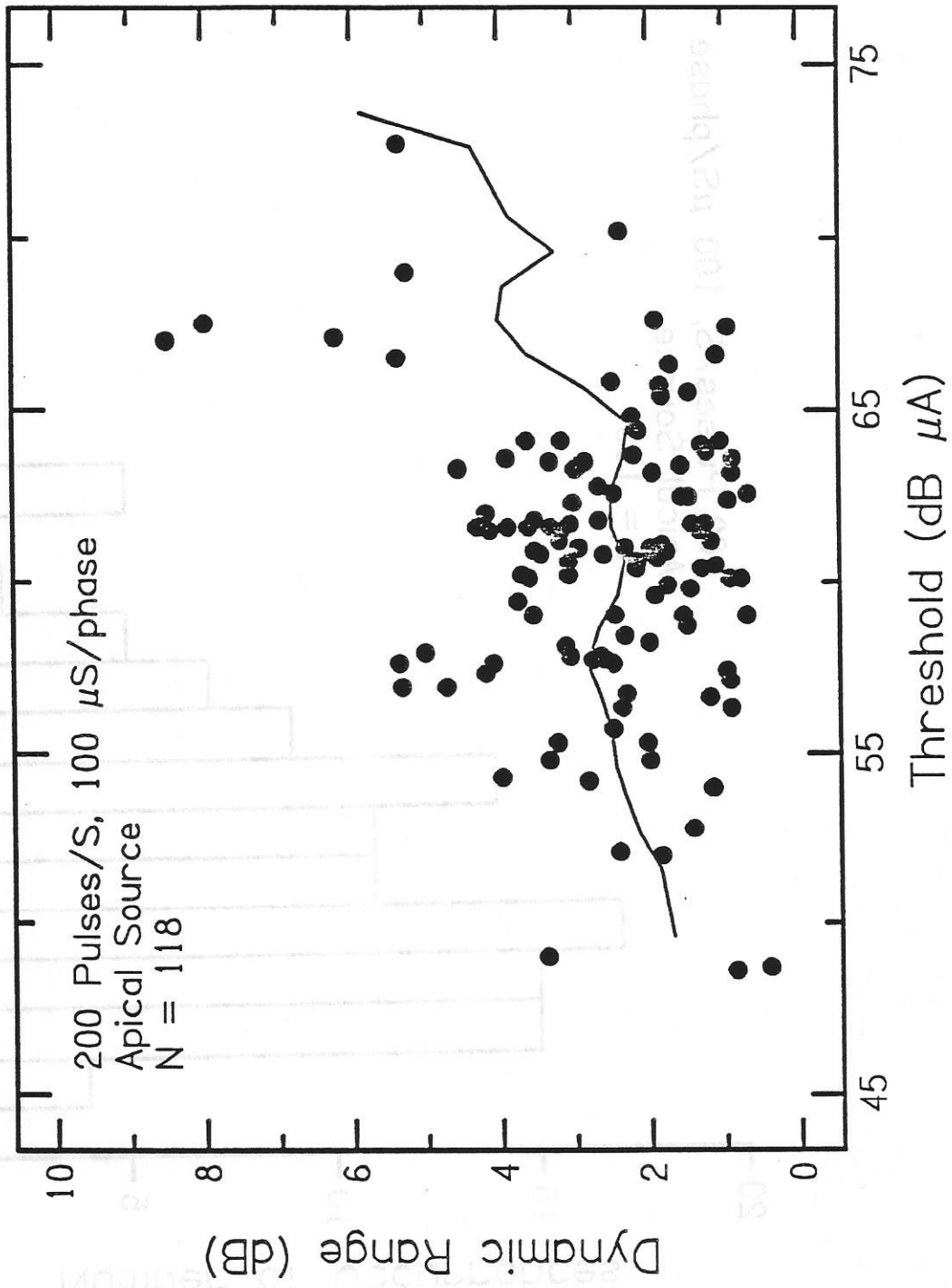
200 Pulses/S, 100 μS/phase
Apical Source
N = 118
Dynamic Range (dB)
0
2
4
6
8
10
45
55
65
75
Threshold (dB μA)

Figure 10

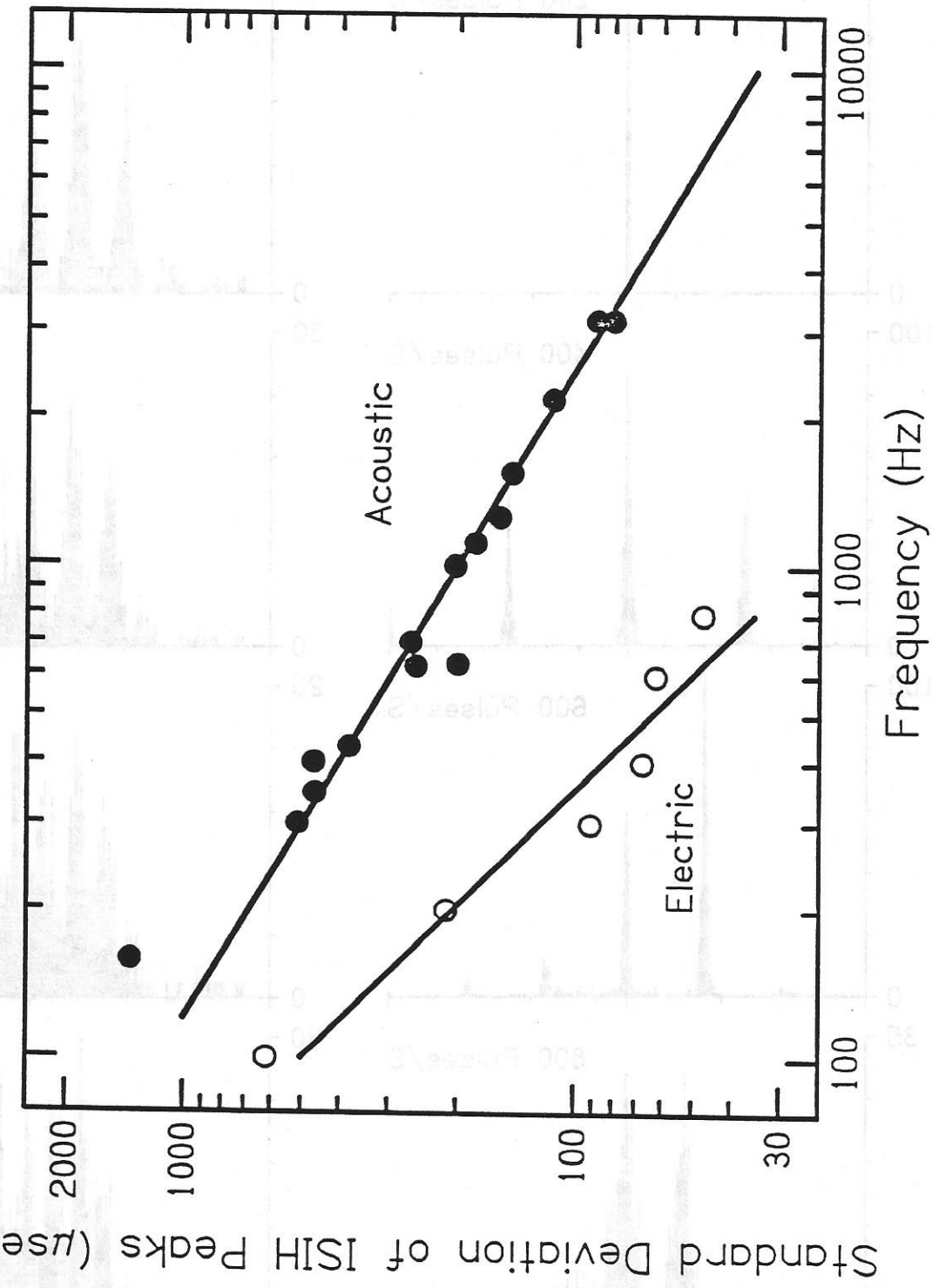
Standard Deviation of ISIH Peaks (μsec)
2000
1000
100
30
100
1000
10000
Frequency (Hz)
Acoustic
Electric

Figure 11

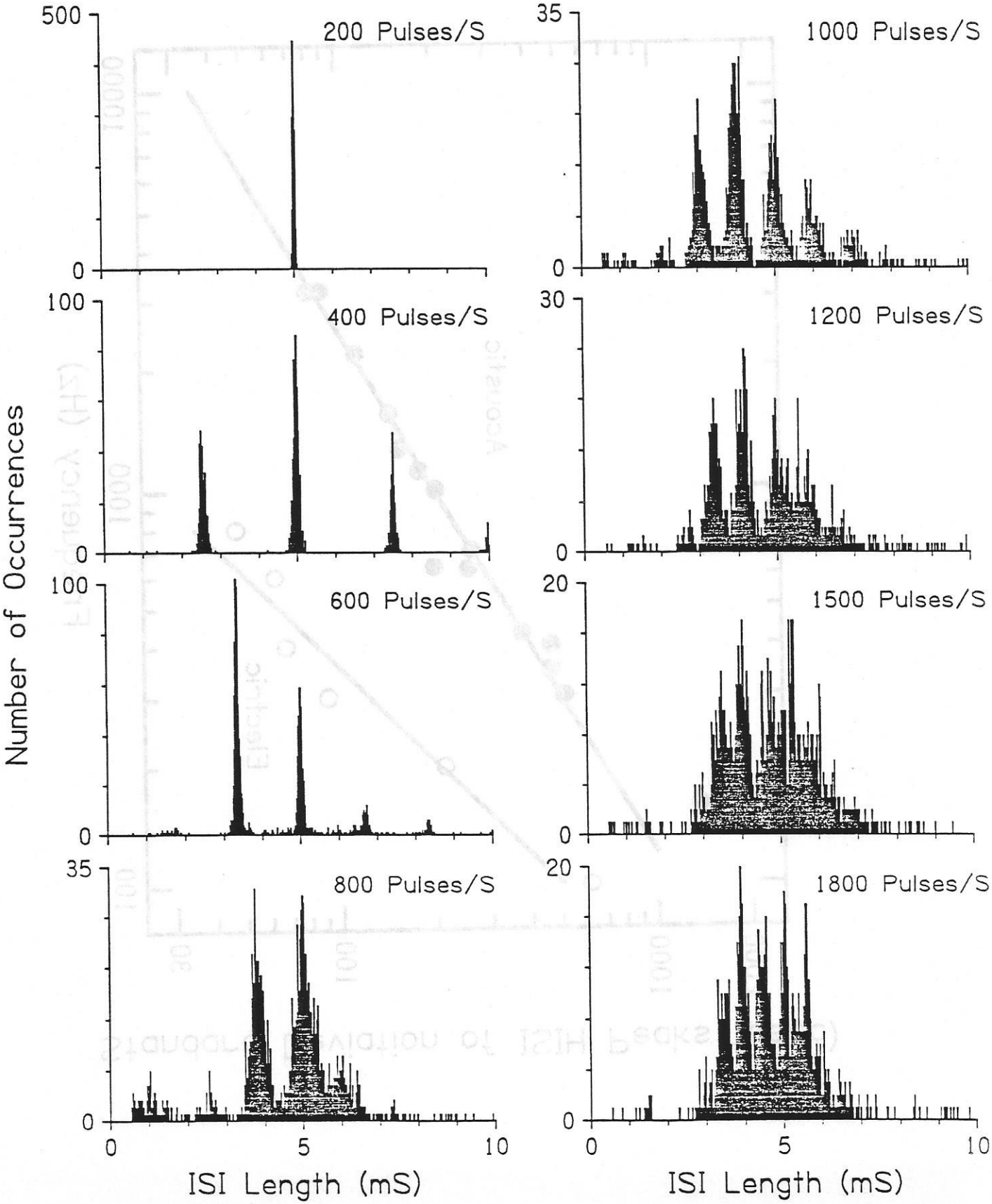
500
200 Pulses/S
0
35
1000 Pulses/S
0
100
400 Pulses/S
0
30
1200 Pulses/S
0
100
600 Pulses/S
0
20
1500 Pulses/S
0
35
800 Pulses/S
0
20
1800 Pulses/S
0
0
5
10
ISI Length (mS)
0
5
10
ISI Length (mS)
Number of Occurrences

Figure 12

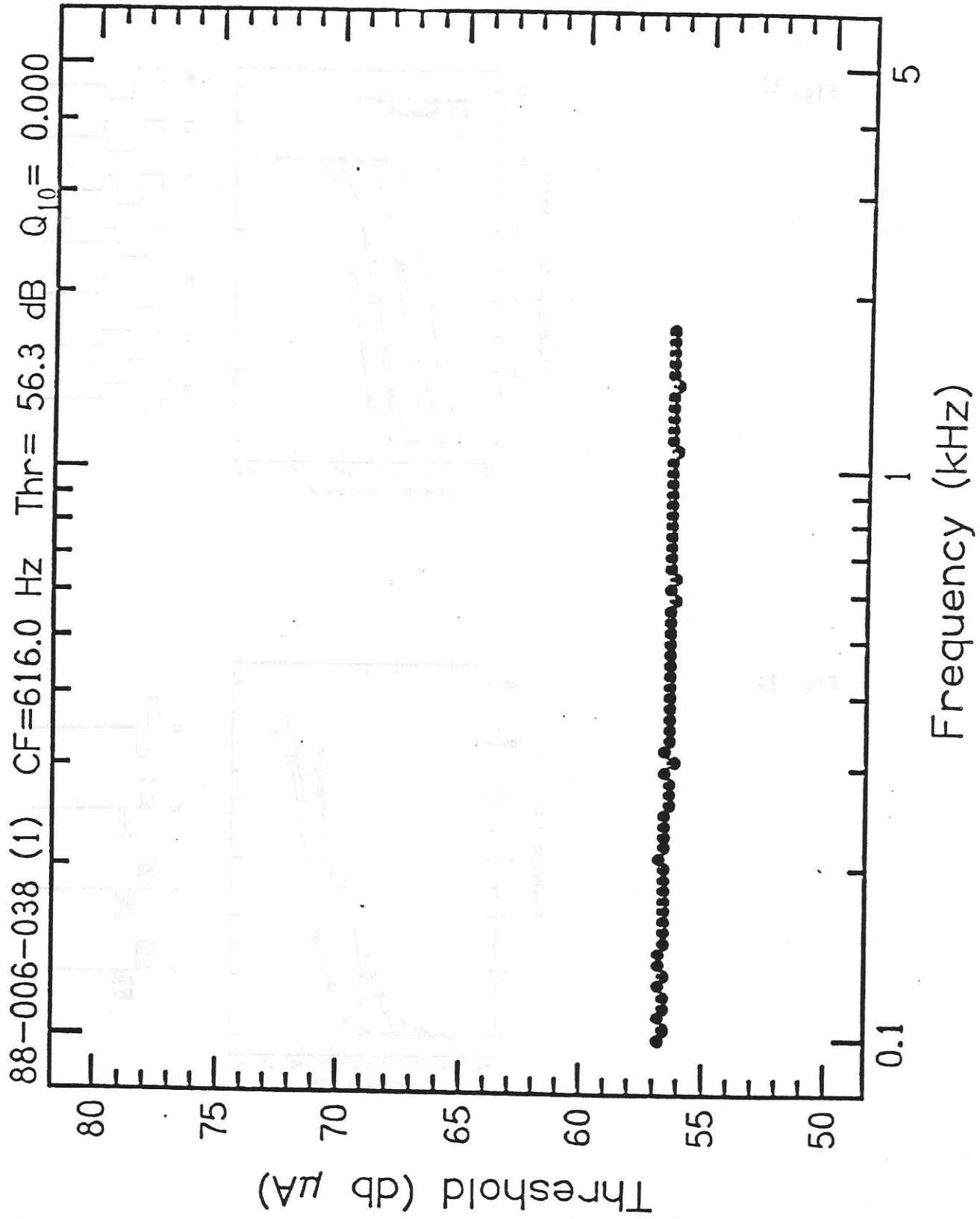
88-006-038 (1) CF=616.0 Hz Thr= 56.3 dB Q10= 0.000
Threshold (db μA)
80
75
70
65
60
55
50
0.1
1
5
Frequency (kHz)

Fig. 13

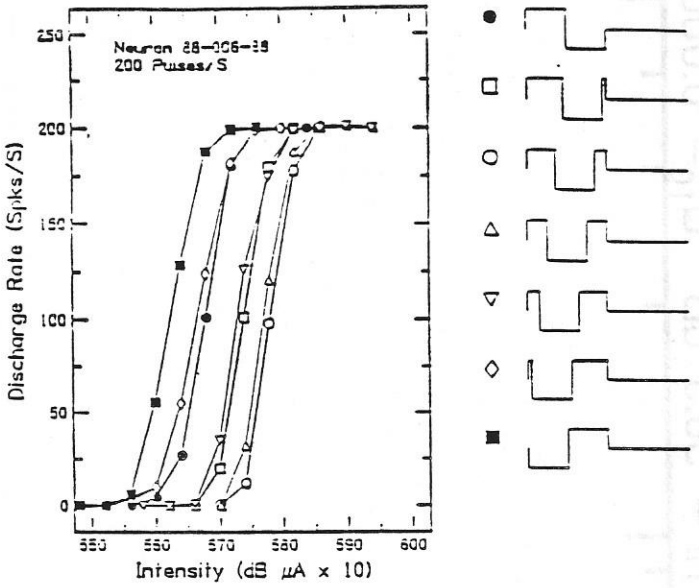
Neuron 28-106-18
200 Pulses/S
Discharge Rate (Spks/S)
Intensity (dB μA x 10)

Fig. 14

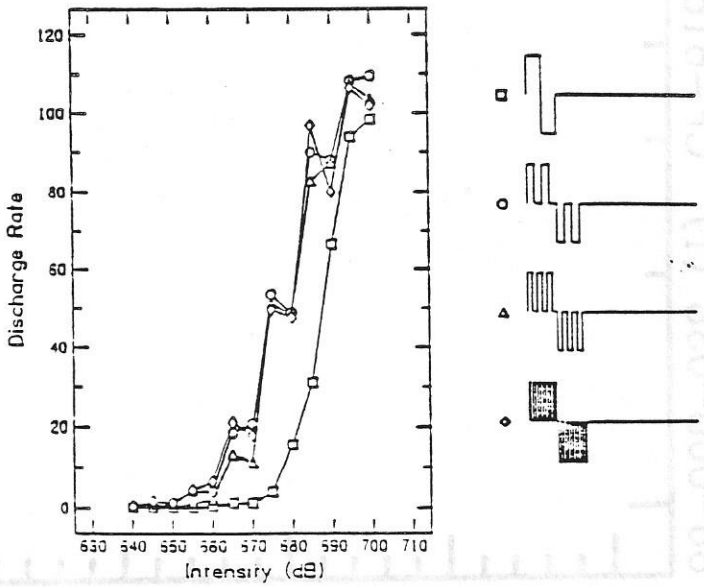
Discharge Rate
Intensity (dB)

Javel, Eric

Fig. 15

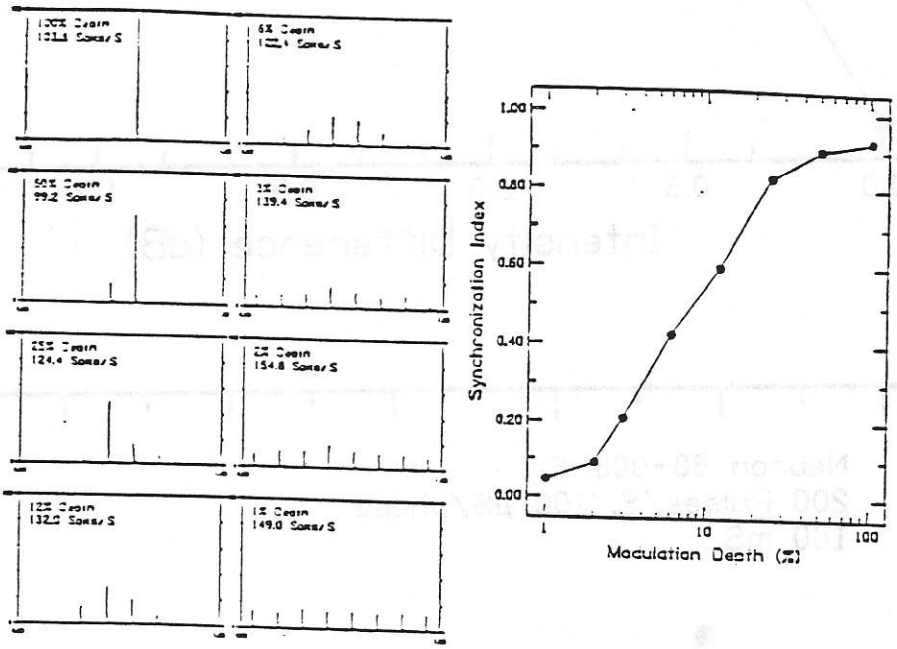

Figure 16

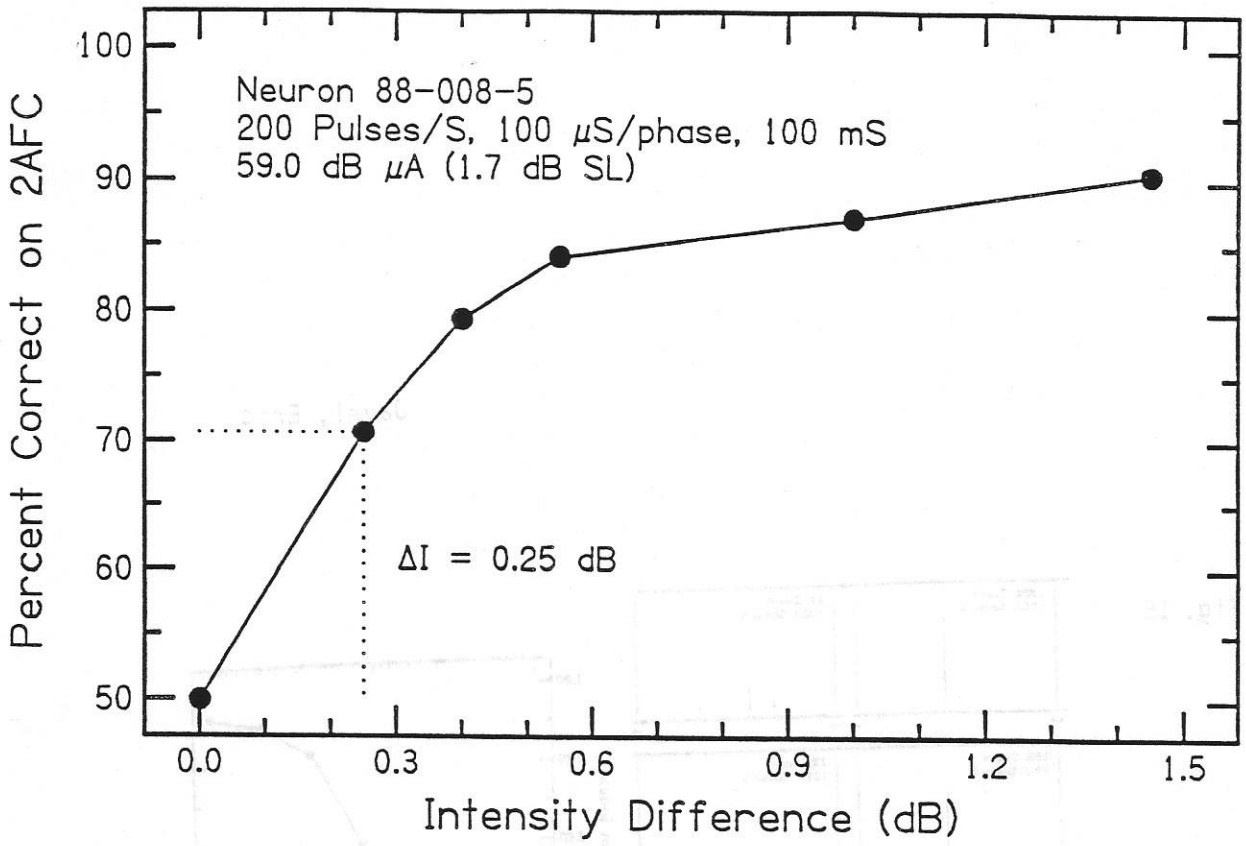
Neuron 88-008-5
200 Pulses/S, 100 μS/phase, 100 mS
59.0 dB μA (1.7 dB SL)
ΔI = 0.25 dB
Percent Correct on 2AFC
100
90
80
70
60
50
0.0
0.3
0.6
0.9
1.2
1.5
Intensity Difference (dB)

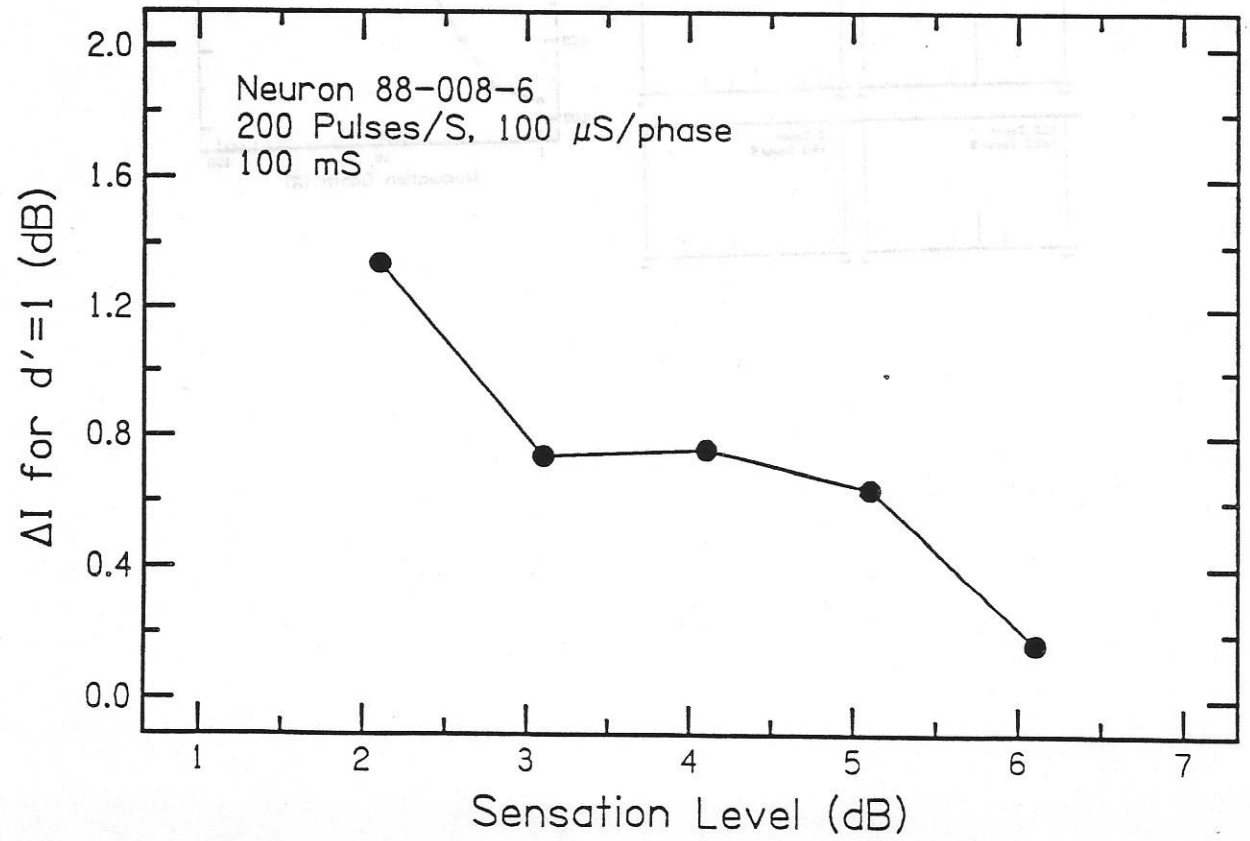
Neuron 88-008-6
200 Pulses/S, 100 μS/phase
100 mS
ΔI for d'=1 (dB)
2.0
1.6
1.2
0.8
0.4
0.0
1
2
3
4
5
6
7
Sensation Level (dB)

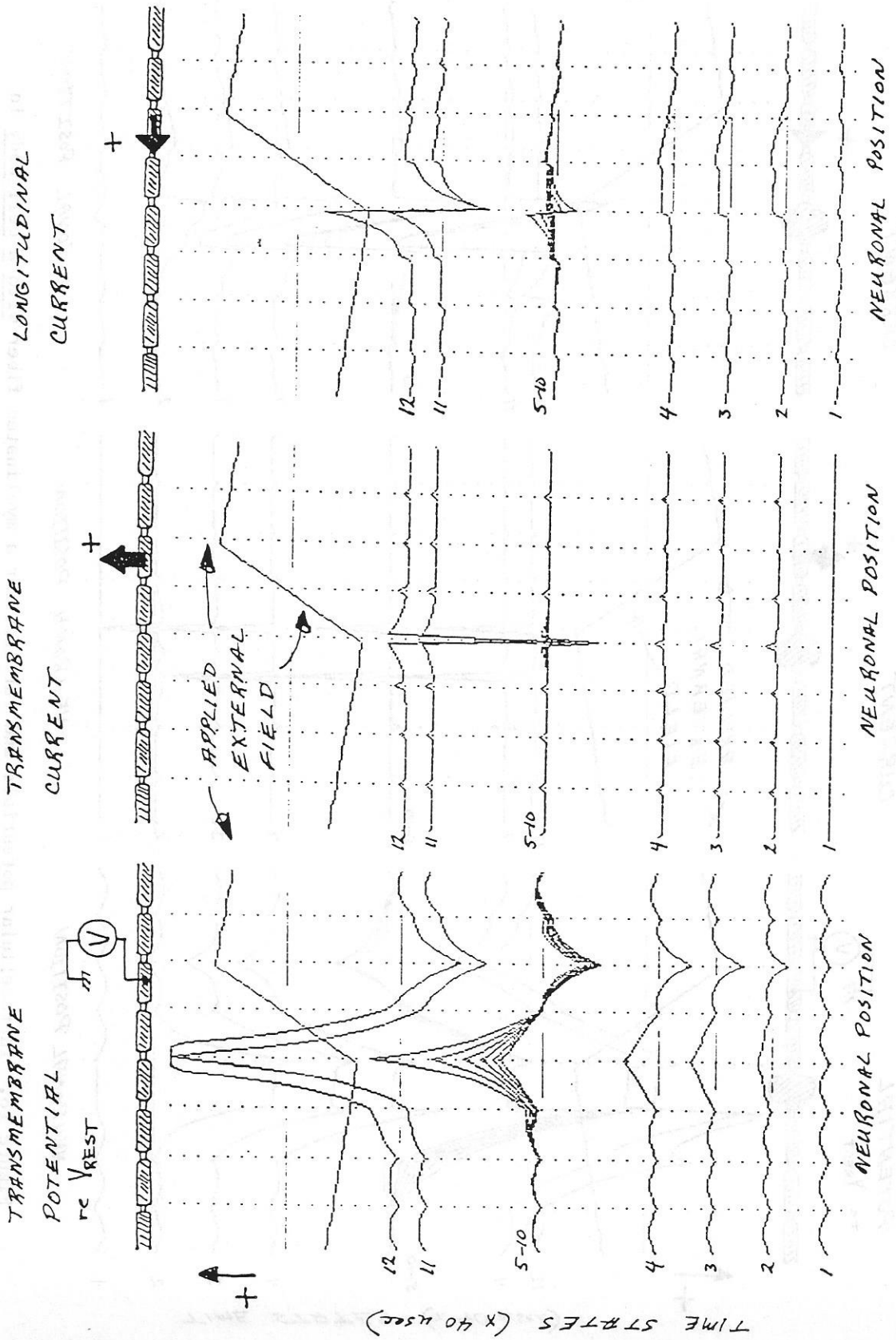

Figure 17. Intracellular potentials and currents for a myelinated fiber in response to extracellular stimulation.

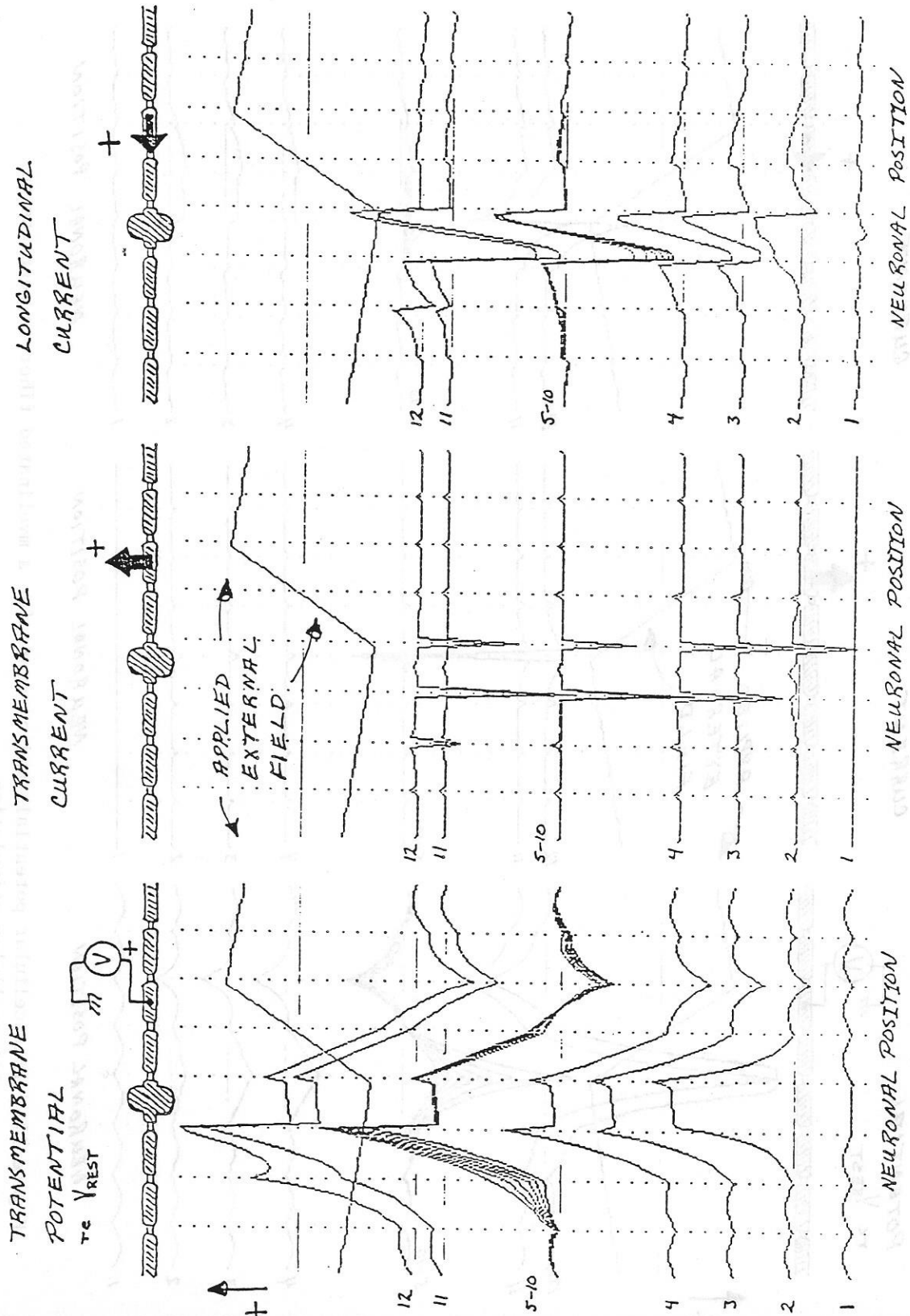

Figure 18. Intracellular potentials and currents for a myelinated fiber with a cell body in response to extracellular stimulation.

Same conditions as for Figure 17, but with cell body added.

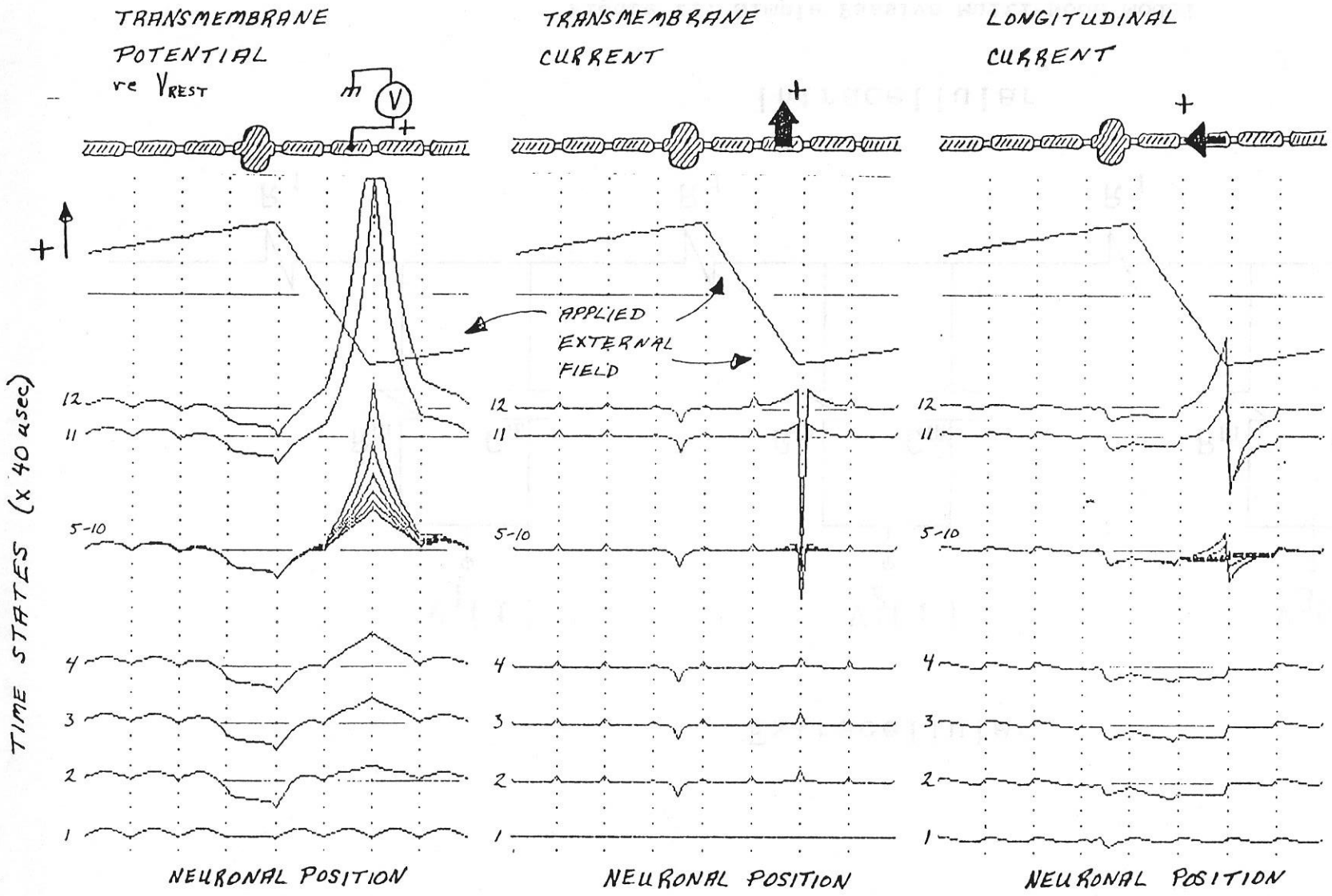

Figure 19. Intracellular potentials and currents for a myelinated fiber with a cell body in response to extracellular stimulation.

Same conditions as for Figure 18, but with polarity of stimulus reversed.

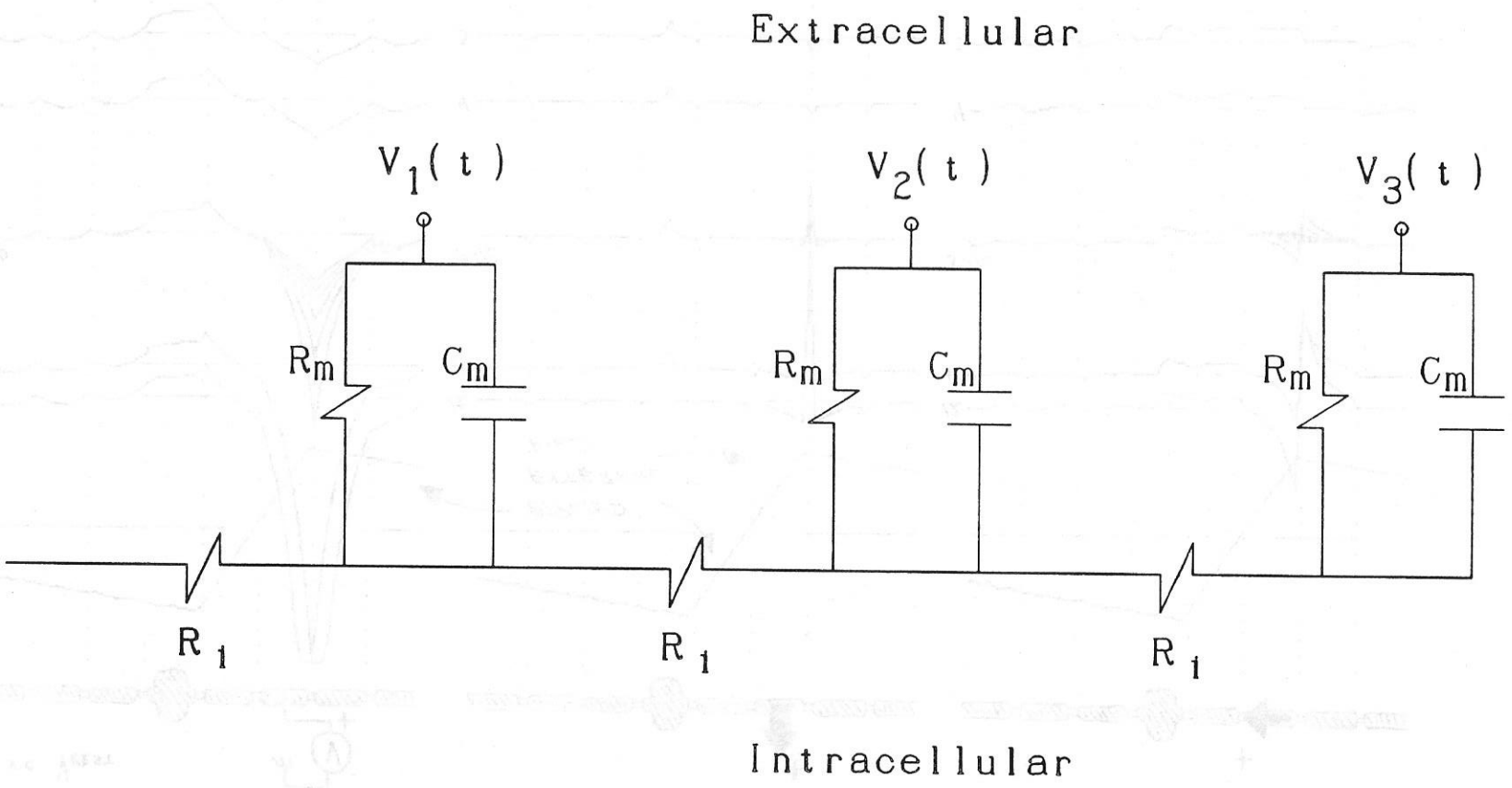

Figure 21. Simple Passive Multi-Node Model

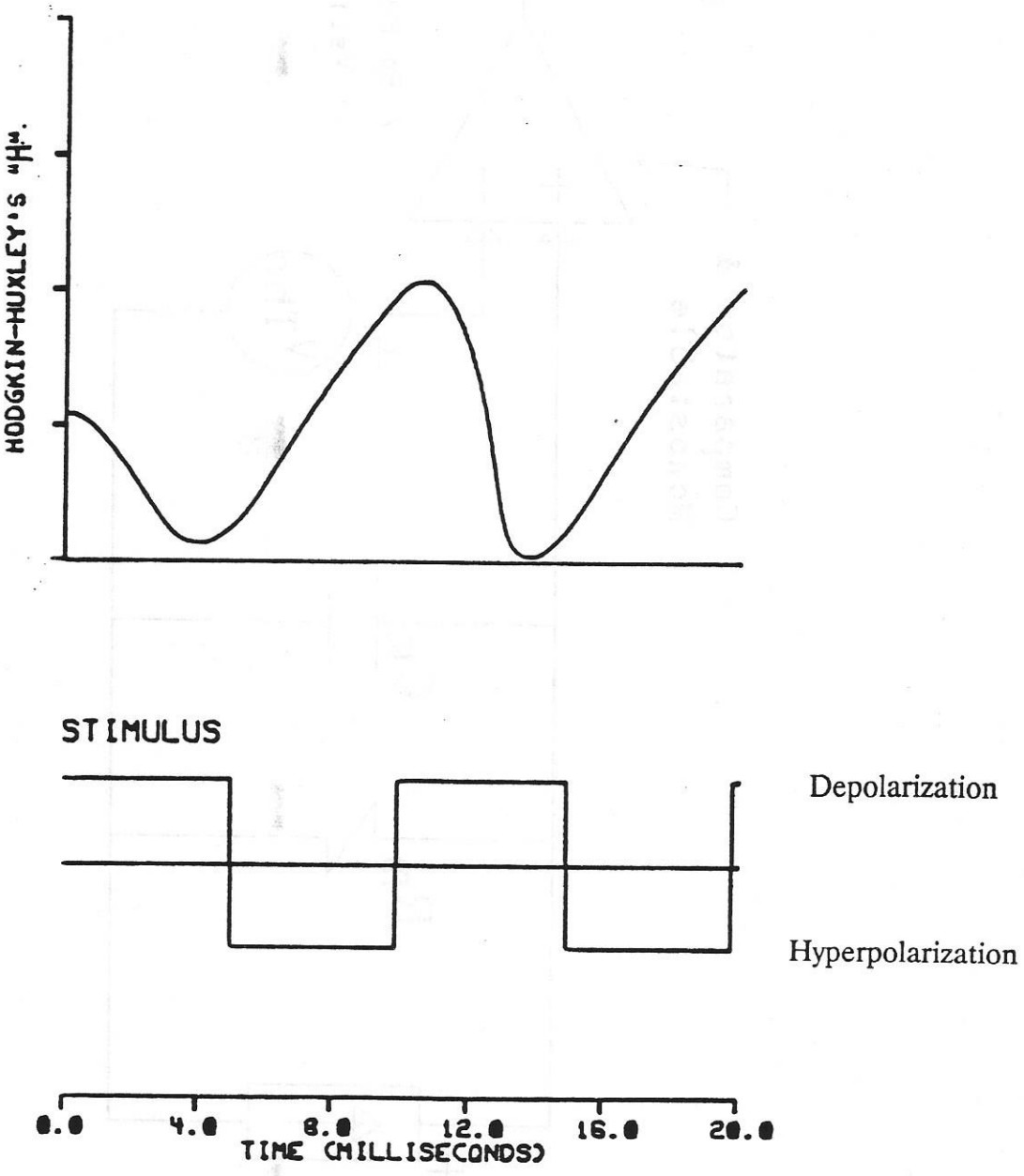

Figure 22 illustrates how "H," the Hodgkin-Huxley deactivation variable, varies after onset of a 100 Hz square-wave pulse train using a controlled current source. "H" is not very large at the onset of the first depolarizing phase of the stimulus. "H" is greatest after rebounding from the hyperpolarization phase of the stimulus. Because "H" must be relatively large for excitation to occur, this rebound effect appears to improve excitability. Note that the H-H model was modified by increasing beta-h four-fold.

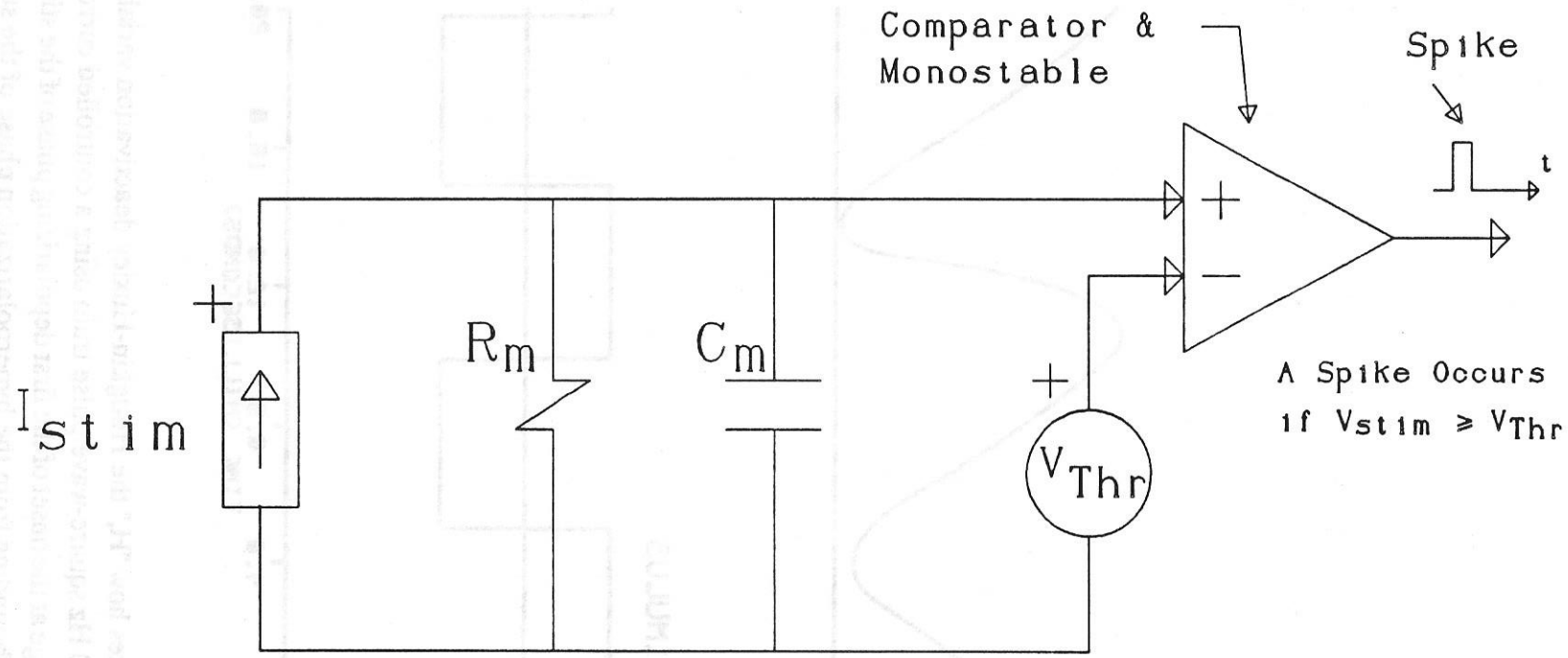

Figure 23. Hill's Model

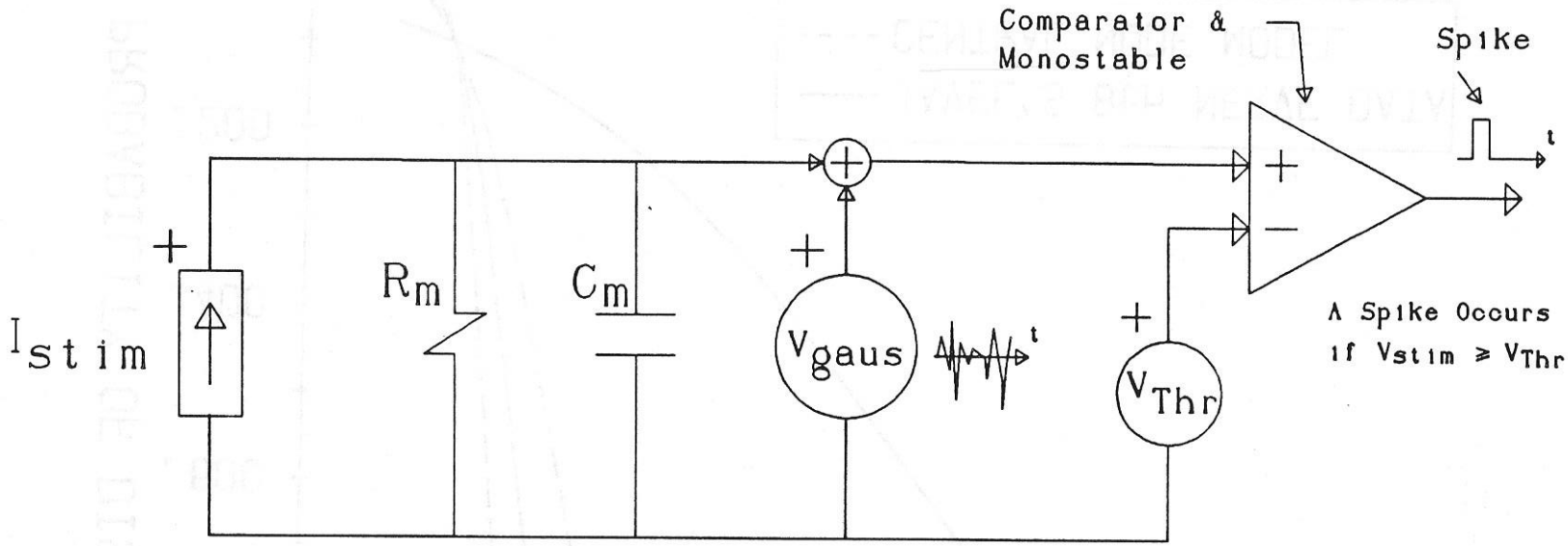

V_{gaus} is a monotonically decreasing function of the node's surface area.

Figure 24. Hill's Model Modified to Generate Stochastic Behavior.

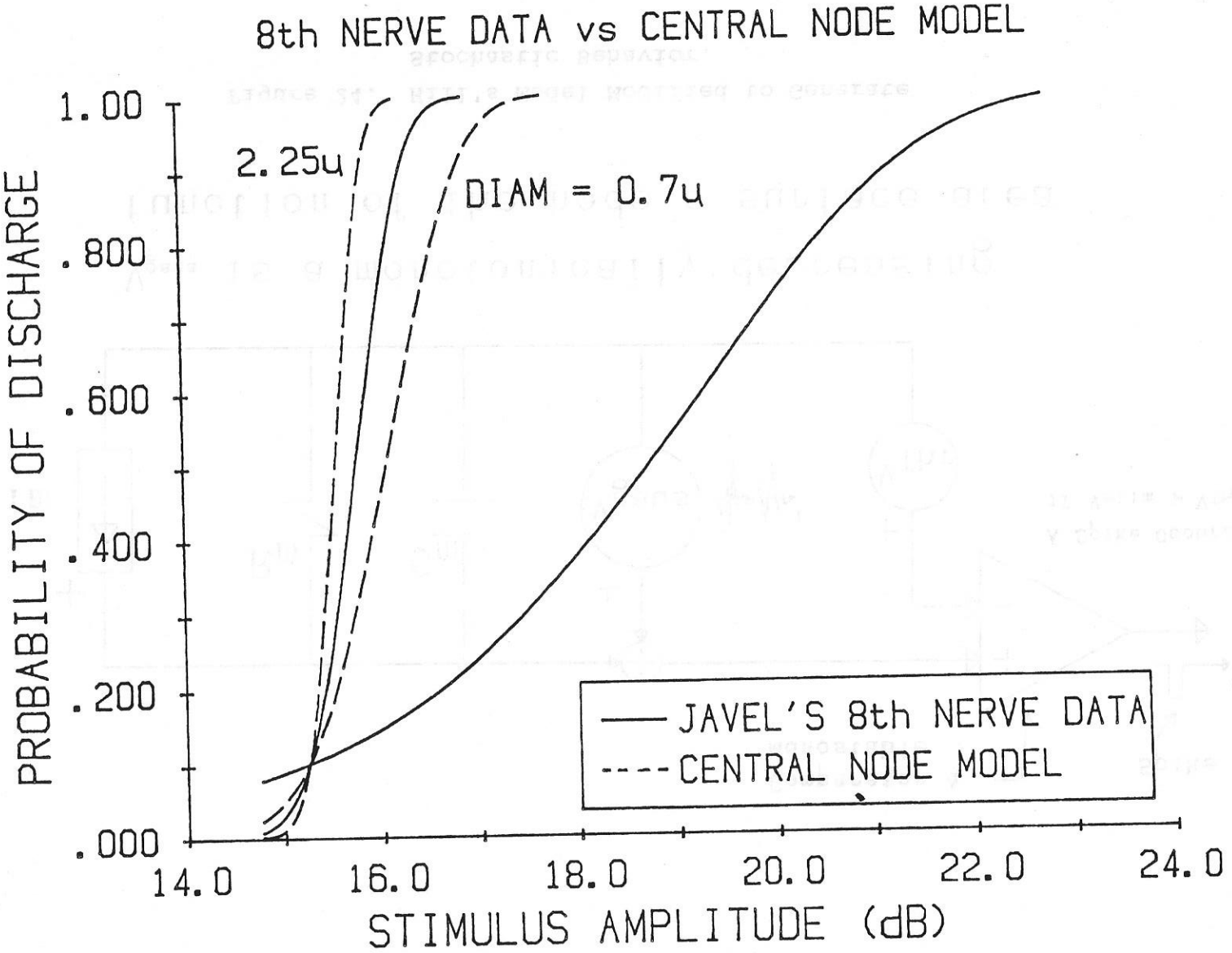

Figure 25. Probability of Discharge vs. Stimulus Amplitude for Central Node Model Compared to Javel's Eighth Nerve Data.

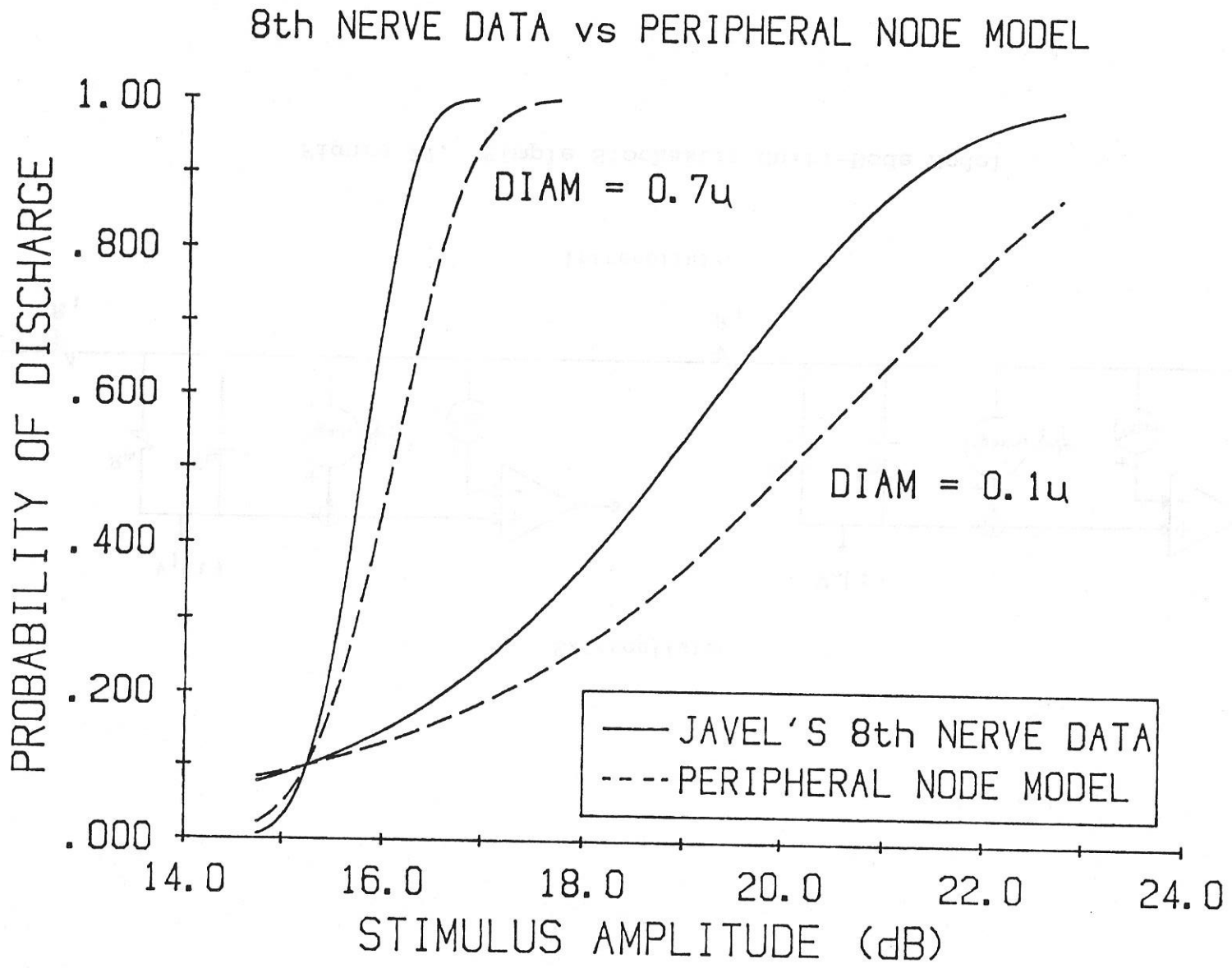

Figure 26. Probability of Discharge vs. Stimulus Amplitude for Peripheral Node Model Compared to Javel's Eighth Nerve Data.

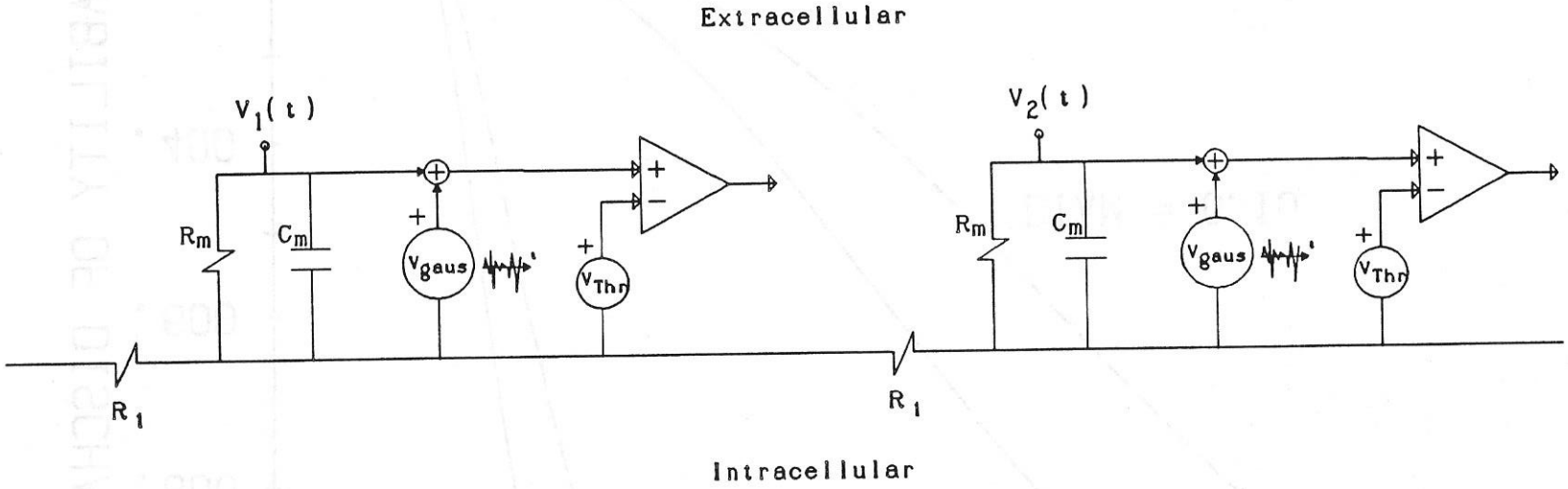

Figure 27. Simple Stochastic Multi-Node Model